

Local-Global Context Aware Transformer for Language-Guided Video Segmentation

Chen Liang, Wenguan Wang, *Senior Member, IEEE*, Tianfei Zhou,
Jiaxu Miao, Yawei Luo, and Yi Yang, *Senior Member, IEEE*

Abstract—We explore the task of language-guided video segmentation (LVS). Previous algorithms mostly adopt 3D CNNs to learn video representation, struggling to capture long-term context and easily suffering from visual-linguistic misalignment. In light of this, we present LOCATER (local-global context aware Transformer), which augments the Transformer architecture with a finite memory so as to query the entire video with the language expression in an efficient manner. The memory is designed to involve two components – one for persistently preserving global video content, and one for dynamically gathering local temporal context and segmentation history. Based on the memorized local-global context and the particular content of each frame, LOCATER holistically and flexibly comprehends the expression as an adaptive query vector for each frame. The vector is used to query the corresponding frame for mask generation. The memory also allows LOCATER to process videos with linear time complexity and constant size memory, while Transformer-style self-attention computation scales quadratically with sequence length. To thoroughly examine the visual grounding capability of LVS models, we contribute a new LVS dataset, A2D-S⁺, which is built upon A2D-S dataset but poses increased challenges in disambiguating among similar objects. Experiments on three LVS datasets and our A2D-S⁺ show that LOCATER outperforms previous state-of-the-arts. Further, we won the 1st place in the Referring Video Object Segmentation Track of the 3rd Large-scale Video Object Segmentation Challenge, where LOCATER served as the foundation for the winning solution. Our code and dataset are available at: <https://github.com/leonnop/Locater>.

Index Terms—Language-guided Video Segmentation, Multi-modal Transformer, Memory Network.

1 INTRODUCTION

LANGUAGE-GUIDED video segmentation (LVS) [1], also known as language-queried video actor segmentation [2], aims to segment a specific object/actor in a video referred by a linguistic phrase. LVS is a challenging task as it delivers high demands for understanding whole video content and diverse language concepts, and, most essentially, comprehending alignments between linguistic and spatio-temporal visual clues at pixel level. Till now, popular LVS solutions are mainly upon FCN-style architectures with different visual-linguistic information fusion modules, such as dynamic convolution [2], cross-modal attention [3], [4].

Though impressive, most existing LVS solutions fail to fully exploit the global video context and the connection between global video context and language descriptions. This is because they usually adopt 3D CNNs [5] for video representation learning. Due to the heavy computational cost and locality nature of 3D kernels, many algorithms can only gather limited information from short video clips (with 8-/16-frame length [2], [3], [6]–[8]) but discard long-term temporal context, which, however, is crucial for LVS task. First, due to the underlying *low-level video processing* challenges such as object occlusion, appearance change and fast motion, it is hard to segment the target referent safely by only considering short-term temporal context [9]–[11]. Second, from a perspective of *high-level visual-linguistic seman-*



Fig. 1. **Our main idea.** Previous LVS models are mainly built upon 3D CNNs, bounded by the local observations from short durations. They thus fail to identify the target referent in the early stage beyond the ‘fall’ event. In contrast, LOCATER is fully aware of both local and global context, enabling a holistic understanding of entire video content and correctly grounding the phrase over the whole video.

tics understanding, short-term temporal context is insufficient for reaching a complete understanding of video content and struggles for tackling complex activity related phrases. As shown in Fig. 1, given the description of “a boy is skiing on the snow and suddenly falling . . .”, the target skier cannot be identified unless with a holistic understanding of the video content, as the ‘fall’ event happens in the second half of the video.

To cope with these temporal and cross-modal challenges posed in LVS task, we propose a new model, named as LOCATER (local-global context aware Transformer). Build-

- C. Liang, W. Wang, J. Miao, Y. Luo, and Y. Yang are with ReLER, CCAI, Zhejiang University. (Email: {leonliang, yangyics}@zju.edu.cn, {wenguanwang.ai,yaweiluo329}@gmail.com, jiaxu.miao@yahoo.com)
- T. Zhou is with ETH Zurich. (Email: ztfei.debug@gmail.com)
- Corresponding author: Yi Yang

ing upon Transformer encoder-decoder architecture [12], LOCATER first utilizes self-attention to enhance per-frame representations with intra-frame visual context and linguistic features. To further incorporate temporal cues into per-frame representation, LOCATER builds an external, *finite* memory, which encodes multi-temporal-scale context and also bases content retrieve on the attention operation. This makes LOCATER a fully attentional model, yet with greatly reduced space and computation complexities.

In particular, the external memory has two components: i) the former is to persistently memorize global temporal context, *i.e.*, highly compact descriptors summarized from frames sampled over the entire span of a video; ii) the latter is to online gather local temporal context and segmentation history, from past segmented frames. The global memory is maintained unchanged during the whole segmentation procedure while the local memory is dynamically updated with the segmentation processes. Hence, LOCATER gains a holistic understanding of video content and captures temporal coherence, leading to contextualized visual representation learning. Conditioned on the stored context and particular content of one frame, LOCATER vividly interprets the expression by adaptively attending to informative words, and forms an expressive query vector that specifically suits that frame. The specific query vector is then used to query corresponding contextualized visual feature for mask decoding.

With such a memory design, LOCATER is capable of comprehensively modeling temporal dependencies and cross-modal interactions in LVS, and processing arbitrary length videos with low time complexity $\mathcal{O}(N)$ and constant space cost $\mathcal{O}(1)$. In contrast, Transformer-style self-attention requires to maintain all $\mathcal{O}(N^2)$ cross-frame dependencies. In addition, we introduce a deeply supervised learning strategy that feeds supervision signal into intermediate layers of LOCATER, for easing training and boosting performance.

We further notice that in A2D-S [2], the most popular LVS dataset, a large portion of videos only contain very few but obvious objects/actors, making such task trivial. To address this limitation, we synthesize A2D-S⁺, a *harder* dataset, from A2D-S. Each video in A2D-S⁺ is either selected or created to contain several semantically similar objects through a semi-automatic contrasting sampling [13] process. It doubles the dataset difficulty in terms of the number of grounding-required examples per video, while with a negligible cost of human labour.

The contributions can be summarized into three folds:

- We propose the pilot work that tackles LVS task with a memory augmented, fully attentional Transformer framework. Several essential designs (*i.e.*, finite memory, progressive cross-modal fusion, contextualized query embedding, deeply supervision) significantly facilitate the network learning and finally lead to impressive performance.
- The finite memory enables elegant long-term memorization and extraction of cross-modal context, while in the meantime, getting rid of the unaffordable space and computation cost brought by the quadratic complexity of the conventional attention in Transformers.
- We alleviate the excess of trivial cases in the current most popular LVS benchmark, *i.e.*, A2D-S, through introducing a *harder* synthesized dataset with little human effort.

We empirically demonstrate that LOCATER consistently surpasses existing state-of-the-arts across three popular benchmark datasets (*i.e.*, 3.6%/5.9%/1.1% on A2D-S [2] (§5.1)/J-HMDB-S [2] (§5.2)/R-YTVOS [4] (§5.3) in mIoU/mIoU/ $\mathcal{J}\&\mathcal{F}$) and also performs robust on our challenging A2D-S⁺ dataset (§5.5). Moreover, based on LOCATER, we ranked 1st place in the Referring Video Object Segmentation (RVOS) track in the 3rd Large-scale Video Object Segmentation Challenge [14] (YTB-VOS₂₁), outperforming the runner-up by a large margin (*e.g.*, 11.3% in $\mathcal{J}\&\mathcal{F}$; see §5.6). Further, we conduct a series of diagnostic experiments on several variants of LOCATER, verifying both the efficacy and efficiency of our core model designs (§5.7).

2 RELATED WORK

To offer necessary background, we review literature in LVS (§2.1), and discuss relevant work in other areas (§2.2-2.7).

2.1 Language-guided Video Segmentation (LVS)

Studies of LVS are initiated by [2], [15]. With the theme of efficiently capturing the multi-modal nature of the task, existing efforts investigate different visual-linguistic embedding schemes, such as capsule routing [8], dynamic convolution [2], [6], [7], and cross-modal attention [3], [15], [16]. Owing to the difficulty in handling variable duration of videos, existing algorithms are mainly built on 3D CNNs, suffering from an intrinsic limitation in modeling dependencies among distant frames [17]–[21]. To remedy this issue, we exploit self-attention to gather cross-modal and temporal cues in a holistic and efficient manner. This is achieved by augmenting Transformer architecture with an explicit memory, which gathers and stores both global and local temporal context with learnable operations. Although [4] also enjoys the advantage of the outside memory, it does not consider global video context and requires multi-round complicated inference with a *heuristic* memory update rule. In essence, we formulate the task in an encoder-decoder attention framework, instead of following the widely-used CNN-style architecture. Two concurrent works [22], [23], inspired by the query-based paradigm in object detection [24] and instance segmentation [25], formulate LVS as a sequence prediction problem and introduce Transformers for querying object sequences. Though effective, they have to translate the whole video as input tokens. In contrast, with the aid of the external memory, LOCATER yields comparable performance with improved efficiency.

2.2 Referring Image Segmentation (RIS)

As the counterpart of LVS in image domain, RIS has longer research history, dating back to the work [26] of Hu and others in 2016. Primitive solutions directly fuse concatenated language and image features with a segmentation network to infer the referent mask [26]–[30]. More recent approaches focus on designing modules to promote visual-linguistic interactions, *e.g.*, cross-modal attention [31], [32], progressive dual-modal encoding [33], linguistic structure [34]–[36].

2.3 Referring Expression Comprehension (REC)

REC is to localize linguistic phrases in images (phase grounding) or videos (language-guided object tracking, LOT), in a form of bounding box. The majority of studies, to date, follow a *two-stage* procedure to select the best-matching region from a set of bounding box proposals [37]–[44]. Despite their promising results, the performance of two-stage methods is capped by the speed and accuracy of the proposal generator. Alternatively, a few recent works resort to a *single-stage* paradigm, which embeds linguistic features into one-stage detectors, and directly predicts the bounding box [45]–[47]. Compared with REC, LVS is more challenging since it requires pixel-level joint video-language understanding. As for LOT, it is an emerging research domain [48]. Existing solutions typically equip famous trackers with a language grounding module [48]–[50]. Note that there are many differences between LOT and LVS: i) they explain phrases with different visual constituents (pixel *vs* tight bounding box); ii) LOT adopts first-frame oriented phrases due to its tracking nature, while LVS is more aware of video understanding, *i.e.*, considering arbitrary objects and unconstrained referring expressions [15].

2.4 Semi-automatic Video Object Segmentation (SVOS)

SVOS aims to selectively segment video objects based on first-frame masks. LVS also has a close connection with SVOS, as it replaces the expensive pixel-level intervention with easily acquired linguistic guidance. Depending on the utilization of test-time supervision, current SVOS models can be categorized into three classes [1]: i) *online fine-tuning based* methods first train a generic segmentation network and then fine-tune it with the given masks [51], [52]; ii) *propagation based* methods use the previous frame mask to infer the current one [53]–[57]; and iii) *matching based* methods classify each pixel’s label according to its similarity to the annotated target [58]–[60]. Although some recent matching based SVOS approaches [60]–[62] also leverage memory to reuse past segmentation information, we focus on a multi-modal task, and enhance Transformer self-attention with a fixed size memory to address the efficiency issue in modeling intra- and inter-modal long-term dependencies.

2.5 Transformer in Vision-Language Tasks

The remarkable successes of Transformer [12] in NLP spur increasing efforts applying Transformer for vision-language tasks, *e.g.*, video captioning [63], text-to-visual retrieval [64], [65], visual question answering [66], and temporal language localization [67]. For generating coherent captions, [63] also utilizes memory to better summarize history information. However, our target task, LVS, requires fine-grained grounding on the spatio-temporal visual space, and our LOCATER exploits local and global video context as well as segmentation history in a comprehensive and efficient manner. Transformer-based *pretrained* models also showed great potential in joint image-language embedding [68]–[75]. Some other efforts were made towards unsupervised video-language representation learning [76], [77], while they still often utilize 3D CNNs for video content encoding.

2.6 Transformer in Visual Referring Tasks

Concurrent to our work, only a handful of attempts apply Transformer-style models for LVS [22], [23], RIS [78], and REC [79]–[82]. Compared with these efforts, our approach is unique in several aspects, including memory design, language-guided progressive encoding, contextualized query embedding, and deep supervision strategy.

2.7 Neural Networks with External Memory

Modeling structures within sequential data has long been considered a foundational problem in machine learning. Recurrent networks (RNNs) [83], *e.g.*, LSTM [84], GRU [85], as a traditional class of methods, have been shown Turing-Complete [86] and successfully applied into a wide range of relevant fields, *e.g.*, machine translation [87], and video recognition [88], [89]. However, due to the limited capacity of the latent network states, they struggle for long-term context modeling. To address this limitation, researchers [90] enrich RNNs’ dynamic storage updates with external memory design, whose long-term memorization/reasoning with explicit storage manipulations earns remarkable success in robot control [91]–[93], language modeling [94]–[96], *etc.*

Drawing inspiration from these novel designs, we equip LOCATER with an external memory. This allows for persistent and precise information storage, as well as flexible manipulations using learnable read/write operations. Hence such memory-augmented architecture well supports long-term modeling, which is critical for LVS.

3 METHODOLOGY

Given a video $\mathcal{I} = \{I_t \in \mathbb{R}^{W \times H \times 3}\}_{t=1}^{N_t}$ with N_t frames and a language expression $E = \{e_w\}_{w=1}^{N_w}$ with N_w words, LVS is to predict a sequence of masks $\{S_t \in \{0, 1\}^{W \times H}\}_{t=1}^{N_t}$ that determine the referent in each frame. Our LOCATER can *efficiently* query the *entire* video with the expression, by exploiting global and local temporal context through an external memory. We first review the preliminary for Transformer (§3.1), and then elaborate our model design (§3.2).

3.1 Preliminary: Transformer Architecture

The core of Transformer [12] is the attention mechanism. Given the query embedding $\mathbf{F}^q \in \mathbb{R}^{N_q \times D_k}$, key embedding $\mathbf{F}^k \in \mathbb{R}^{N_v \times D_k}$ and value embedding $\mathbf{F}^v \in \mathbb{R}^{N_v \times D_v}$, the output of a *single-head attention* layer is computed as:

$$\mathcal{F}_{\text{ATT}}(\mathbf{F}^q, \mathbf{F}^k, \mathbf{F}^v) = \text{softmax}\left(\frac{\mathbf{F}^q \mathbf{F}^{k\top}}{\sqrt{D_k}}\right) \mathbf{F}^v. \quad (1)$$

Combining several paralleled single-head attention, one can derive *multi-head attention*. In Transformer, each encoder block has two layers, *i.e.*, multi-head self-attention (MSA) and a multi-layer perceptron (MLP). MSA is a variant of multi-head attention, where the query, key and value are from the same source. Each encoder block is formulated as:

$$\begin{aligned} \mathbf{X}' &= \text{LN}(\mathbf{X} + \mathcal{F}_{\text{MSA}}(\mathbf{X})), \\ \mathbf{Y} &= \text{LN}(\mathbf{X}' + \mathcal{F}_{\text{MLP}}(\mathbf{X}')), \end{aligned} \quad (2)$$

where residual connection and layer-normalization are applied; \mathbf{X} and \mathbf{Y} are the input and output, respectively.

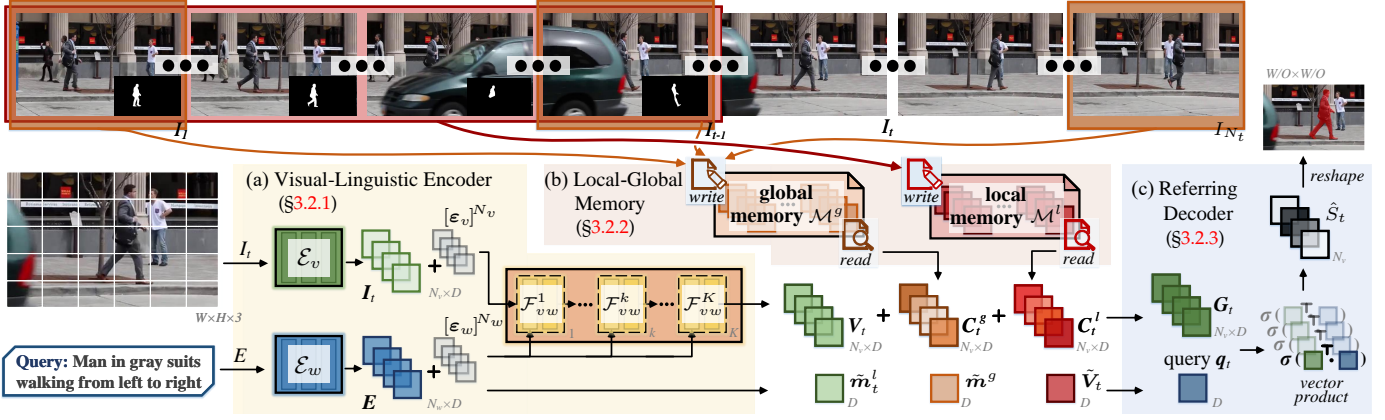


Fig. 2. **Illustration of our LOCATER.** Building upon Transformer encoder-decoder architecture, LOCATER maintains a finite memory to collect and retain both global and local temporal context. By referencing the memory, LOCATER can reach a holistic understanding of video content and query the entire video with the expression, with linear computation complexity and constant storage consumption. See §3.2 for details.

The decoder block has a similar structure. A multi-head attention layer is first adopted, where a specific query embedding is generated to gather information from the encoder side, with the output of corresponding encoder block as key and value embeddings.

Despite the strong expressivity, applying Transformer to LVS is not trivial. As the self-attention function (*cf.* Eq. 1) comes with quadratic time and space complexity, letting Transformer capture all the intra- and inter-modal relations is not feasible. To address the efficiency issue, some studies exploit sparse attention [97], [98], linear attention [99], [100], and recurrence [101]–[103]. With a similar spirit, we develop LOCATER that specifically focuses on LVS and models temporal and cross-modal dependencies with constant size memory and time complexity linear in sequence length.

3.2 Local-Global Context Aware Transformer

Given the input video $\{I_t\}_t$ and language expression E , our LOCATER mainly consists of three parts (see Fig. 2): **i)** a *visual-linguistic encoder* (§3.2.1) that gradually fuses the linguistic embedding E into visual embedding I_t and generates a language-enhanced visual feature V_t for each frame I_t ; **ii)** a *local-global memory* (§3.2.2) that gathers diverse temporal context from $\{I_t\}_t$ so as to render V_t as a contextualized feature G_t and comprehend the expression E into an expressive yet frame-specific query vector q_t ; and **iii)** a *referring decoder* (§3.2.3) that queries G_t with q_t for mask prediction \hat{S}_t .

3.2.1 Visual-Linguistic Encoder

As illustrated in Fig. 2 (a), the visual-linguistic encoder first extracts visual and linguistic features from each frame and the referring expression respectively, and then aggregates them into a compact, language-enhanced visual feature, through self-attention.

Single-Modality Encoders. For each frame $I_t \in \mathbb{R}^{W \times H \times 3}$, a visual encoder \mathcal{E}_v is adopted to generate a raw visual embedding, *i.e.*, $I_t = \mathcal{E}_v(I_t) \in \mathbb{R}^{N_v \times D}$. Here I_t is a sequence of D -dimensional embeddings of N_v image patches, *i.e.*, $I_t = \{I_{t,p} \in \mathbb{R}^D\}_{p=1}^{N_v}$, where each patch is of $O \times O$ pixels and $N_v = WH/O^2$. At the same time, we forward the referring

expression E into a language encoder \mathcal{E}_w to get the corresponding linguistic embedding, *i.e.*, $E = \mathcal{E}_w(E) \in \mathbb{R}^{N_w \times D}$.

Cross-Modality Encoder. To fuse heterogeneous features of each frame image and language expression early, we devise a cross-modality encoder \mathcal{E}_{vw} . It adopts a Transformer encoder architecture, that captures all the correlations between image patches and language words, with several cascaded blocks. Specifically, the k -th module \mathcal{F}_{vw}^k is formulated as:

$$F_1^k = \mathcal{F}_{vw,1}^k([F_2^{k-1} + [\epsilon_v]^{N_v}, E + [\epsilon_w]^{N_w}]) \in \mathbb{R}^{N_v \times D}, \quad (3)$$

$$F_2^k = \mathcal{F}_{vw,2}^k(F_1^k) \in \mathbb{R}^{N_v \times D}, \quad (4)$$

where $\epsilon_v \in \mathbb{R}^D$ and $\epsilon_w \in \mathbb{R}^D$ are learnable token type vectors that indicate whether an input token is from frame image or phrase. $[\cdot, \cdot]$ indicates concatenation operation and $[\cdot]^{N_v}$ copies its input vector N times before concatenation. $\mathcal{F}_{vw,1}^k$ and $\mathcal{F}_{vw,2}^k$ are implemented as the Transformer encoder block (*cf.* §3.1), and $F_2^0 = I_t$. In k -th module, the first block $\mathcal{F}_{vw,1}^k$ takes $(k-1)$ -th module's output, F_2^{k-1} , and the text feature, E , as inputs, and conducts cross-modal fusion. Then it feeds its output, F_1^k , into the second block, $\mathcal{F}_{vw,2}^k$, for further refinement. Note that, for $\mathcal{F}_{vw,1}^k$, only the first N_v output visual embeddings are preserved, while the last N_w linguistic outputs are directly discarded.

With global operations, each module enriches every patch embedding with both the textual context and intra-frame context. By stacking K attention-based modules, \mathcal{E}_{vw} repeats such visual feature enhancement process K times, addressing the heterogeneity of visual and linguistic cues, and finally outputting a language-enhanced visual feature $V_t \in \mathbb{R}^{N_v \times D}$ for each frame I_t .

3.2.2 Local-Global Memory

Although V_t yields a powerful multi-modal representation, it is less suitable for LVS, as it is computed for each frame I_t individually without accounting for temporal information. Directly using all the video patches $\{I_{t,p}\}_{t,p}$ as the visual tokens of the cross-modality attention encoder \mathcal{E}_{vw} will cause unaffordable computational and memory costs, since the complexity of self-attention computation scales quadratically with the sequence length (*cf.* §3.1). We thus frame a

local-global memory module \mathcal{M} , which helps LOCATER to capture the temporal context in an efficient manner.

Specifically, \mathcal{M} has two parts, *i.e.*, \mathcal{M}^l and \mathcal{M}^g (Fig. 2 (b)), for capturing local and global temporal context, respectively. Both the global memory $\mathcal{M}^g = \{\mathbf{m}_n^g \in \mathbb{R}^D\}_{n=1}^{N_g}$ and local memory $\mathcal{M}^l = \{\mathbf{m}_n^l \in \mathbb{R}^D\}_{n=1}^{N_l}$ have a fixed capacity, which is much smaller than the number of patches in \mathcal{I} , *i.e.*, $N_g \ll N_v N_t$ and $N_l \ll N_v N_t$. Each memory cell \mathbf{m}^g (\mathbf{m}^l) is a highly summarized visual state from the whole video (several past frames), empowering LOCATER with a holistic understanding of video content. With learnable operations, the memory collects informative spatio-temporal context, dynamically interacts with the memory contents, and selectively determines which content should be preserved. This is in stark contrast to standard Transformer that stores immutable key and value vectors of all the tokens, causing huge storage size. LOCATER also uses the attention mechanism to retrieve its local-global memory, making it a fully attentional model.

Global Memory. To construct the global memory \mathcal{M}^g , we first evenly sample a set of $N_{t'}$ frames from the whole video, which are supportive enough for comprehensive video content understanding, due to the redundancy among frames. Then we adopt a learnable *write* controller to compress and store these sampled frames into \mathcal{M}^g as the global context. Specifically, given a sampled frame $I_{t'}$ with its language-enhanced visual feature $\mathbf{V}_{t'} = \{\mathbf{V}_{t',p} \in \mathbb{R}^D\}_{p=1}^{N_v}$, for each patch p , we update every memory cell in parallel:

$$\begin{aligned} \mathbf{c}_p^g &= \mathcal{F}_c^g(\mathbf{V}_{t',p}, [\mathbf{m}_n^g]_n) = \mathbf{W}_c^g[\mathbf{V}_{t',p}, \mathcal{F}_{\text{AP}}([\mathbf{m}_n^g]_n)] \in \mathbb{R}^D, \\ \mathbf{o}_p^g &= \mathcal{F}_o^g(\mathbf{c}_p^g, [\mathbf{m}_n^g]_n) = [\sigma(\mathbf{c}_p^{g\top} \mathbf{W}_o^g \mathbf{m}_n^g)]_n \in [0, 1]^{N_g}, \\ \mathbf{m}_n^g &\leftarrow \mathcal{F}_{\text{AP}}([o_{n,p}^g \cdot \mathbf{c}_p^g + (1 - o_{n,p}^g) \cdot \mathbf{m}_n^g]_p) \in \mathbb{R}^D, \end{aligned} \quad (5)$$

where \mathcal{F}_{AP} refers to the average pooling operation, $\sigma(\cdot)$ is sigmoid activation, $[\cdot]_n$ indicates concatenating over variable n . $\mathbf{W}_c^g \in \mathbb{R}^{D \times 2D}$ and $\mathbf{W}_o^g \in \mathbb{R}^{D \times D}$ are learnable parameters, and $[\mathbf{m}_n^g]_n$ is initialized as learnable states. Iteratively, \mathcal{F}_c^g creates a candidate \mathbf{c}_p^g for memory update, based on $\mathbf{V}_{t',p}$ and $[\mathbf{m}_n^g]_n$; \mathcal{F}_o^g returns a gate vector $\mathbf{o}_p^g = [o_{n,p}^g]_{n=1}^{N_g}$ according to the uniqueness of \mathbf{o}_p^g w.r.t. all the memory slots $[\mathbf{m}_n^g]_n$; $o_{n,p}^g$ controls how much information to retain from prior state in n -th memory slot. In this way, the write controller learns to collect global context into \mathcal{M}^g and obviate redundant and noisy information.

After processing all the $N_{t'}$ sampled frames, the global memory \mathcal{M}^g is constructed and maintained unchanged during the whole segmentation process of \mathcal{I} . Thus LOCATER can pay continuous attention to global context, so as to better interpret long-term or complex activity related phrases (*e.g.*, “a boy is skiing and suddenly falling” in Fig. 1) and handle video processing challenges (*e.g.*, occlusion, fast motion, *etc.*).

Local Memory. For the local memory \mathcal{M}^l , it is constructed and updated on-the-fly. Specifically, given the last segmented frame I_{t-1} , with corresponding local memory state $\mathcal{M}_{t-1}^l = \{\mathbf{m}_{t-1,n}^l \in \mathbb{R}^D\}_{n=1}^{N_l}$, language-enhanced visual feature $\mathbf{V}_{t-1} = \{\mathbf{V}_{t-1,p} \in \mathbb{R}^D\}_{p=1}^{N_v}$ and predicted segmentation mask $\hat{S}_{t-1} = \{s_{t-1,p} \in [0, 1]\}_{p=1}^{N_v}$ (*i.e.*, a sequence of patch segments), the new memory state \mathcal{M}_t^l for current frame I_t is obtained, again, by a learnable *write* controller applied onto

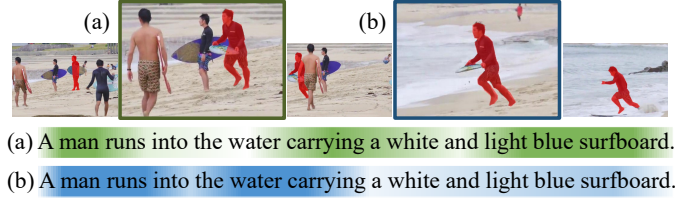


Fig. 3. **Attention visualization** of frame-specific queries (Eq. 10).

each memory state in parallel, like in Eq. 5:

$$\begin{aligned} \mathbf{c}_p^l &= \mathcal{F}_c^l([\mathbf{V}_{t-1,p}, \mathbf{s}_{t-1,p}], [\mathbf{m}_{t-1,n}^l]_n) \in \mathbb{R}^D, \\ \mathbf{o}_p^l &= \mathcal{F}_o^l(\mathbf{c}_p^l, [\mathbf{m}_{t-1,n}^l]_n) \in [0, 1]^{N_l}, \\ \mathbf{m}_{t,n}^l &= \mathcal{F}_{\text{AP}}([o_{n,p}^l \cdot \mathbf{c}_p^l + (1 - o_{n,p}^l) \cdot \mathbf{m}_{t-1,n}^l]_p) \in \mathbb{R}^D, \end{aligned} \quad (6)$$

where $\mathbf{s}_{t-1,p} \in \mathbb{R}^D$ is a trainable segmentation mask embedding. It is obtained by applying a small FCN over \hat{S}_{t-1} . As a similar operation in Eq. 5, the write controller learns to gather short-term context from past segmented frames and selectively update the contents of the local memory in a frame-by-frame manner.

With \mathcal{M}^l , LOCATER can access and leverage local temporal context to comprehend simple action-related descriptions (*e.g.*, “a woman is running”), and generate temporally coherent results with the aid of segmentation history.

Contextualized Visual Embedding. LOCATER next enriches the linguistic-enhanced visual feature \mathbf{V}_t of I_t with local-global context, by looking up its current memory $\mathcal{M}_t = \{\mathcal{M}^g, \mathcal{M}_t^l\} = \{\mathbf{m}_{t,n}\}_{n=1}^{N_g+N_l}$. An attention-based *read* operator is used to retrieve context from the memory \mathcal{M}_t :

$$\begin{aligned} \mathbf{c}_t^g &= \mathcal{F}_{\text{ATT}}(\mathbf{V}_t, [\mathbf{m}_n^g]_n, [\mathbf{m}_n^g]_n) \in \mathbb{R}^{N_v \times D}, \\ \mathbf{c}_t^l &= \mathcal{F}_{\text{ATT}}(\mathbf{V}_t, [\mathbf{m}_{t,n}^l]_n, [\mathbf{m}_{t,n}^l]_n) \in \mathbb{R}^{N_v \times D}, \end{aligned} \quad (7)$$

where \mathbf{c}_t^g and \mathbf{c}_t^l refer to the gathered global and local temporal context, respectively. Then we generate a contextualized visual embedding \mathbf{G}_t for frame I_t :

$$\mathbf{G}_t = \mathbf{V}_t + \mathbf{c}_t^g + \mathbf{c}_t^l \in \mathbb{R}^{N_v \times D}. \quad (8)$$

With this local-global memory-induced attention operation, \mathbf{G}_t encodes multi-modal information and rich temporal context, which is used in the decoder for querying the referent.

3.2.3 Referring Decoder

Contextualized Query Embedding. The local-global memory can not only enable contextualized visual embedding, but also help better parse the language expression. We first derive three compact vectors, *i.e.*, $\tilde{\mathbf{V}}_t \in \mathbb{R}^{1 \times D}$, $\tilde{\mathbf{m}}^g \in \mathbb{R}^{1 \times D}$ and $\tilde{\mathbf{m}}_t^l \in \mathbb{R}^{1 \times D}$, from \mathbf{V}_t , \mathcal{M}^g and \mathcal{M}_t^l , respectively, to summarize visual context in different temporal scales:

$$\tilde{\mathbf{V}}_t = \mathcal{F}_{\text{AP}}([\mathbf{V}_{t,p}]_p), \tilde{\mathbf{m}}^g = \mathcal{F}_{\text{AP}}([\mathbf{m}_n^g]_n), \tilde{\mathbf{m}}_t^l = \mathcal{F}_{\text{AP}}([\mathbf{m}_{t,n}^l]_n), \quad (9)$$

where \mathcal{F}_{AP} indicates the average pooling operation, defined in Eq. 5. Then, LOCATER interprets the expression $\mathbf{E} = \{\mathbf{E}_w \in \mathbb{R}^{1 \times D}\}_{w=1}^{N_w}$ as a compact query vector \mathbf{q}_t , by using visual context guided attention to adaptively emphasize informative words:

$$\begin{aligned} a_{t,w} &= \text{softmax}_w([\tilde{\mathbf{V}}_t, \tilde{\mathbf{m}}^g, \tilde{\mathbf{m}}_t^l] \mathbf{W}_1) (\mathbf{E}_w \mathbf{W}_2)^\top \in [0, 1], \\ \mathbf{q}_t &= \sum_{w=1}^{N_w} a_{t,w} \cdot \mathbf{E}_w \in \mathbb{R}^{1 \times D}, \end{aligned} \quad (10)$$

where $\mathbf{W}_1 \in \mathbb{R}^{3D \times D}$ and $\mathbf{W}_2 \in \mathbb{R}^{D \times D}$ are learnable parameters, and $[a_{t,w}]_w$ encodes the importance of each word, by taking both temporal visual context, *i.e.*, $\tilde{\mathbf{m}}^g$, $\tilde{\mathbf{m}}^l$, and specific content of frame I_t , *i.e.*, $\tilde{\mathbf{V}}_t$, into account. As shown in Fig. 3, with frame-specific attentions, the generated query vector \mathbf{q}_t is expressive and particularly fits the corresponding frame I_t , instead of previous LVS methods [2], [6], [8], [15] processing all the frames with a fixed query embedding.

Referent Mask Decoding. For mask generation, LOCATER queries the contextualized visual embedding $\mathbf{G}_t = \{\mathbf{G}_{t,p} \in \mathbb{R}^{1 \times D}\}_{p=1}^{N_v}$ with the frame-specific query vector $\mathbf{q}_t \in \mathbb{R}^{1 \times D}$, by computing product distance between query-patch pairs:

$$\hat{s}_{t,p} = \sigma(\mathbf{G}_{t,p} \mathbf{q}_t^\top) \in [0, 1]. \quad (11)$$

In this way, we can obtain a mask sequence $\hat{S}_t = \{\hat{s}_{t,p}\}_{p=1}^{N_v} \in [0, 1]^{N_v}$ that collects all the patch-level responses. Recall that each patch is of $O \times O$ size and $N_v = WH/O^2$. \hat{S}_t is then reshaped into a 2D mask with $W/O \times H/O$ size and bilinearly upsampled to the original image resolution, *i.e.*, $W \times H$, as the final segmentation result for the frame I_t .

Deeply-Supervised Transformer Learning. In practice, we find our Transformer based model is hard to train. Deeply-supervised learning [104], [105], *i.e.*, introducing supervision signals into intermediate network layers, has been shown effective in CNN-based network training. Given the fact that Transformer also has a layer-by-layer architecture, we suppose that deeply-supervised learning can also help ease the learning of our model. To explore this idea, we separately forward the output features $\{\mathbf{F}_2^k\}_{k=1}^K$ of all the K modules in the cross-modality encoder \mathcal{E}_{vw} (Eq. 4), into an auxiliary readout layer. The readout layer is a small MLP followed by sigmoid activation, and learns to predict a segmentation mask. For each training frame I , given the auxiliary outputs $\{\hat{S}_k \in [0, 1]^{W \times H}\}_{k=1}^K$ from \mathcal{E}_{vw} and final segmentation prediction $\hat{S} \in [0, 1]^{W \times H}$, the training loss is:

$$\mathcal{L} = \sum_I (\mathcal{L}_{\text{CE}}(\hat{S}, S) + \lambda \sum_k \mathcal{L}_{\text{CE}}(\hat{S}_k, S)), \quad (12)$$

where \mathcal{L}_{CE} refers to pixel-wise, binary cross-entropy loss, $S \in \{0, 1\}^{H \times W}$ is the ground-truth mask, and λ balances the two terms. Such a learning strategy can better supervise our early-stage cross-modal information fusion (*cf.* §3.2.1).

3.3 Implementation Details

Detailed Architecture. Each video frame I_t is resized to 320×320 , and then patch-wise separated with a patch size of 16, *i.e.*, $O = 16$ and $N_v = 400$, as in [106]. Each language description is fixed to $N_w = 20$ word length, with padding and truncation for the mismatched ones. The visual encoder \mathcal{E}_v is implemented as six Transformer encoder blocks, while the linguistic encoder \mathcal{E}_w is implemented as a bi-LSTM [107] as in [6], [7]. For the cross-modality encoder \mathcal{E}_{vw} , it has $K=3$ modules. The hidden sizes of all the modules are set to $D = 768$. For the global memory \mathcal{M}^g and local memory \mathcal{M}^l , we set the capacity as $N_g = 1.5N_v$ and $N_l = 2N_v$ respectively. Unless otherwise specified, we sample representative frames with an interval of 10 frames to construct \mathcal{M}^g , *i.e.*, $N_{t'} \approx N_t/10$. Related experiments can be found in §5.7.

Training Details. Our model is trained for 30 epochs using Adam optimizer [108] with initial learning rate 4×10^{-5} ,

batch size 32 and weight decay 1×10^{-4} . We adopt polynomial annealing policy [109] to schedule the learning rate. The λ in Eq. 12 is set to 0.4 by default. Random horizontal flipping is employed as data augmentation where video frames are flipped with the corresponding positional description being modified from “right” to “left” and vice versa.

Inference. During inference, for each video, LOCATER first builds the global memory \mathcal{M}^g and maintains it unchanged. Then, LOCATER conducts segmentation in a sequential manner. The local memory \mathcal{M}^l is gradually updated during segmentation. The continuous segmentation prediction mask \hat{S} for each frame I is binarized with a threshold of 0.5.

4 OUR A2D-S+ DATASET

Till now, A2D-S is the most popular LVS dataset. However, in practice, we find that the majority of its `test` videos (459 of 757) only contain one *single* actor. With these trivial cases, such cross-modal task tends to degrade to a single-modal problem of novel object segmentation. Moreover, many of the remaining videos only contain very few objects yet with distinctive semantics. To better examine the visual grounding capability of LVS models, we construct a *harder* dataset – A2D-S+. It consists of three subsets, *i.e.*, A2D-S_M⁺, A2D-S_S⁺, and A2D-S_T⁺, which are all built upon A2D-S but fully aware of the limitation of A2D-S. Specifically, each video in A2D-S+ is selected/created to contain multiple instances of the same object or action category. Thus our A2D-S+ places a higher demand for the grounding ability of LVS models as the distinction among the similar instances is necessary. Next, we will detail the construction process in §4.1 and discuss dataset features and statistics in §4.2.

4.1 Dataset Construction

We first curate videos with multiple actors from A2D-S `test` as the subset A2D-S_M⁺ (A2D-S_{Multiple}⁺). Although each video in A2D-S_M⁺ has multiple instances, most of these instances are with different semantic categories, making the distinction among them relatively easy. To mitigate this, we further create two challenging subsets: A2D-S_S⁺ and A2D-S_T⁺, by employing a contrasting sampling strategy [13], which synthesizes new test samples from videos that contain similar but not exactly the same instances as described by the language expression. Specifically, the contrasting sampling based construction process of A2D-S_S⁺ and A2D-S_T⁺ includes three steps: **i)** parse free-form language descriptions into semantic-roles (*e.g.*, *who* did *what* to *whom*); **ii)** for each query video, sample a video with the description of the same semantic-roles structure as the queried description, but the role is realized by a different noun or a verb; and **iii)** generate a new sample by concatenating the query and sampled videos along the width axis (for A2D-S_S⁺) or time axis (for A2D-S_T⁺).

Semantic-Role Labeling (SRL). We first parse each free-form language description in A2D-S `test` into semantic-roles [110], *i.e.*, given the description, answer the high-level question of “who (Arg0) did what (Verb) to whom (Arg1)

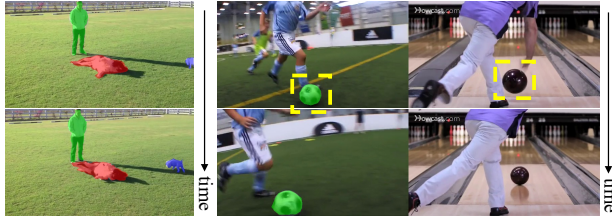
TABLE 1

An example of applying semantic-role labeling to the video description for the construction of $A2D-S_S^+$ and $A2D-S_T^+$. See §4.1 for details.

Original Description: A boy is skiing on the snow and suddenly falling to the ground.		
Verb	Semantic Role labeling	Semantic Groups
is	A boy [Verb: is] skiing on the snow and suddenly falling to the ground.	Filtered out
skiing	[ARG0: A boy] is [Verb: skiing] [ARGM-LOC: on the snow] and suddenly falling to the ground.	A boy skiing on the snow
falling	[ARG0: A boy] is skiing on the snow and [ARGM-TMP: suddenly] [Verb: falling] [ARG2: to the ground].	A boy suddenly falling to the ground
Semantic-Role Labeled Description: (boy, ARG0), (skiing, Verb), (on snow, ARGM-LOC), (suddenly, ARGM-TMP), (falling, Verb), (to ground, ARG2)		
Lemmatized Description: (boy, ARG0), (ski, Verb), (on snow, ARGM-LOC), (suddenly, ARGM-TMP), (fall, Verb), (to ground, ARG2)		

(a) **Black and white dog rolling on the meadow**
The person is watching a dog
Small white dog walking on the right

(b) **White black ball kicked by player and rolling on the grass**
Bowling ball rolling on the track



(a)

(b)

(c)-1 **Baby is crawling the stairs with a man**
Baby crawling through the green tube

(c)-2 **Orange cat is eating from plastic pack**
Dog eating watermelon



(c)

Fig. 4. Representative video examples from our proposed (a) $A2D-S_M^+$, (b) $A2D-S_S^+$, and (c) $A2D-S_T^+$ datasets (§4.1).

at where (ARGM-LOC) and when (ARGM-TMP)¹. In particular, we first use a BERT-based [111] semantic-role labeling model [112] to predict the semantic-roles for each language description. The model is trained on OntoNote5 [113] with PropBank annotations [114]. Then the labeled sentences are further cleaned by: i) removing words without any roles, e.g., “is”, “are”, “a”, “the”; ii) abandoning non-semantic-role labeled sentences; and iii) lemmatization [115]. An example of our semantic-role labeling process is given in Table 1.

Contrasting Sampling. After assigning semantic-roles to language descriptions of $A2D-S_{test}$ videos, we conduct contrasting sampling to find similar but not exactly the same examples, according to their parsed semantic-role structures. Specifically, for each description, we sample one other description from the dataset that contains at least one, but not all, of semantic roles, which are realized with the same phrase. For example, with a description $\{(boy, Arg0), (run, Verb), (on grass, ARGM-LOC)\}$, an eligible sampled description can be $\{(boy, Arg0), (run, Verb), (on snow, ARGM-LOC)\}$. Finally, all sampled example pairs are checked by human for diminishing visual and linguistic confusions.

Concatenation Strategies. For each valid contrasting example pair, two concatenation strategies are adopted to merge them into one video, i.e., concatenating along the space axis as an instance of $A2D-S_S^+$ ($A2D-S_{Spatial}^+$), and along the time axis as an instance of $A2D-S_T^+$ ($A2D-S_{Temporal}^+$). Specifically:

- For $A2D-S_S^+$, videos are concatenated along the width axis exclusively, since height-axis concatenation might violate the natural up-down order in real world, e.g., sky should

1. There are other types of semantic-roles that are not considered in our case, e.g., How (ARGM-MNR), Why (ARGM-CAU), which only applicable for ~1% of the language queries in $A2D-S_{test}$.

TABLE 2

Dataset statistics of $A2D-S_{test}$ and our $A2D-S_{M,S,T}^+$ (§4.2).

Dataset	$A2D-S_{test}$	$A2D-S_M^+$	$A2D-S_S^+$	$A2D-S_T^+$
#Videos	737	257	1,290	1,293
#Queries	1,295	856	1,295	1,295
#Objects/vid	1.76	3.33	5.02	5.13

be on top of grass. The sampled videos are resized to have the same height as the query videos, and truncated or padded to fit the time durations of the query videos.

- For $A2D-S_T^+$, videos are concatenated along the time axis. For a query video with N_t frames, the sampled contrasting video is resized into the same resolution as the query video. There will be $2N_t$ frames in each newly constructed example, in which N_t frames are from the query video, and the other N_t frames are sampled from the contrasting video. For the frames from the contrasting videos, LVS models are expected to predict all-zero masks to indicate that there is no target referent.

Notably, there is no constraint on the concatenation order of videos. By default, we put the query video at the left and ahead, for spatial and temporal concatenation, respectively. We provide representative examples for $A2D-S_{M,S,T}^+$ in Fig. 4.

4.2 Dataset Features and Statistics

Dataset Features. Through the above contrasting sampling process, $A2D-S^+$ has two distinctive characteristics:

- *Dense Grounding-ability Required:* $A2D-S^+$ is manufactured to guarantee that each video does contain multiple se-

TABLE 3
Quantitative results on A2D-S test [2] (§5.1). (*: ViT-B with first 6 layers as backbone. Same for other tables.)

Method	Backbone	Overlap					mAP 0.5:0.95	IoU		FPS
		P@0.5	P@0.6	P@0.7	P@0.8	P@0.9		Overall	Mean	
†Hu <i>et al.</i> [26] [ECCV16]	VGG-16 [116]	34.8	23.6	13.3	3.3	0.1	13.2	47.4	35.0	-
†Li <i>et al.</i> [48] [CVPR17]	VGG-16 [116]	38.7	29.0	17.5	6.6	0.1	16.3	51.5	35.4	-
Gavrilyuk <i>et al.</i> [2] [CVPR18]	I3D [5]	50.0	37.6	23.1	9.4	0.4	21.5	55.1	42.6	-
Wang <i>et al.</i> [3] [ICCV19]	I3D [5]	55.7	45.9	31.9	16.0	2.0	27.4	60.1	49.0	8.64
Wang <i>et al.</i> [7] [AAAI20]	I3D [5]	60.7	52.5	40.5	23.5	4.5	33.3	62.3	53.1	7.18
McIntosh <i>et al.</i> [8] [CVPR20]	I3D [5]	52.6	45.0	34.5	20.7	3.6	30.3	56.8	46.0	-
Ning <i>et al.</i> [6] [IJCAI20]	I3D [5]	63.4	57.9	48.3	32.2	8.3	38.8	66.1	52.9	5.42
Hui <i>et al.</i> [16] [CVPR21]	I3D [5]	65.4	58.9	49.7	33.3	9.1	39.9	66.2	56.1	8.07
Yang <i>et al.</i> [19] [BMVC21]	ResNet-101 [117]	61.1	55.9	48.6	34.2	12.0	-	67.9	52.9	-
LOCATER	*ViT-B [106]	70.9	64.0	52.5	35.1	10.1	42.8	69.0	59.7	10.1
MTTR [23] [CVPR22]	Video-Swin-T [118]	75.4	71.2	63.8	48.5	16.9	46.1	72.0	64.0	6.69
ReferFormer [22] [CVPR22]	Video-Swin-T [118]	76.0	72.2	65.4	49.8	17.9	48.6	72.3	64.1	6.54
LOCATER	Video-Swin-T [118]	76.5	72.8	66.3	49.5	17.1	48.8	71.6	64.2	7.92

mentally similar objects where grounding among them is necessarily required.

- *Low Human-labour Cost:* The entire dataset creation process is semi-automatic so that the human labour cost is greatly reduced. Only a few inevitable efforts have been made to diminish the visual and linguistic ambiguity.

Dataset Statistics. The detailed statistics of A2D-S⁺_{M,S,T} are shown in Table 2. As our A2D-S⁺ is only used to evaluate LVS models, the statistic of A2D-S test is also provided for clear comparison. As seen, compared to A2D-S test, the newly constructed A2D-S⁺_{M,S,T} significantly increase the number of existing semantically similar objects in each video, *i.e.*, 1.76 vs 3.33/5.02/5.13, which together provide a stronger testing bed for evaluating LVS methods.

5 EXPERIMENT

Overview. To thoroughly examine the efficacy of LOCATER, we first report quantitative results on three standard LVS datasets, *i.e.*, A2D Sentences (A2D-S) [2] (§5.1), J-HMDB Sentences (J-HMDB-S) [2] (§5.2), and Refer-Youtube-VOS (R-YTVOS) [4] (§5.3), followed by qualitative results (§5.4). And we further perform experiments on our proposed A2D-S⁺ dataset in §5.5. Then in §5.6, we report the model performance on the RVOS Track in YTB-VOS₂₁ Challenge [14], where our LOCATER based solution achieved the 1st place. Later, in §5.7, we conduct a set of ablative studies to examine the core ideas and essential components of LOCATER. We finally analyse several typical failure modes in §5.8.

Evaluation Criteria. For A2D-S and J-HMDB-S, we follow conventions [2], [3], [6], [7] to use intersection-over-union (IoU) and precision for evaluation. We report *overall IoU* as the ratio of the total intersection area divided by the total union area over testing samples, as well as *mean IoU* as the average IoU of all samples. We also measure precision@*K* as the percentage of testing samples whose IoU scores are higher than an overlap threshold *K*. We report precision at five thresholds ranging from 0.5 to 0.9 and mean average precision (mAP) over 0.50: 0.05: 0.95. For R-YTVOS and YTB-VOS₂₁, we follow their standard evaluation protocols to report the region similarity (\mathcal{J}), contour accuracy (\mathcal{F}) and their average score $\mathcal{J}\&\mathcal{F}$ over all video sequences [119].

5.1 Results on A2D-S Dataset

We first conduct experiments on A2D-S [2], which is the most popular dataset in the field of LVS.

Dataset. A2D-S contains 3,782 videos with 8 action classes performed by 7 actors, and 6,655 actor and action related descriptions. In each video, 5 to 7 frames are provided with segmentation annotations. As in [3], we use 3,017/737 split for train/test, and ignore the 28 unlabeled videos.

Quantitative Performance. Table 3 reports the comparison results of LOCATER against 3D CNN based methods and two latest fully attentional works on the A2D-S test. For fair comparisons with the concurrent competitors [22], [23], we report the model performance with the strong Video-Swin-T [118] backbone. As seen, LOCATER yields state-of-the-art performance for all metrics when compared with 3D CNN based methods. Concretely, it advances the SOTA in mAP by 2.9%, Mean IoU by 3.6%, Overall IoU by 2.8%, and also produces great improvements in terms of precision scores under all overlap thresholds. Equipped with the strong Video-Swin-T backbone, LOCATER achieves comparable or even better performance than the contemporary Transformer based methods [22], [23]. For completeness, we report here the standard deviations of the best performed variants (Row 13): ± 0.354 and ± 0.518 in terms of mIoU and oIoU. These experimental results well demonstrate the superiority of LOCATER on local-global semantics understanding brought by the memory design.

Runtime Analysis. Table 3 reports the efficiency comparison with several famous methods, including four FCN-style models [3], [6], [7], and two latest fully attentional models [22], [23]. For fairness, we conduct runtime analysis on a video clip of 36 frames with resolution 512×512 and a text sequence of 20 words length. The window size of 3D CNN/Transformer backbones, *i.e.*, I3D [5] and Video-Swin-T [118], are all set to 16. The inference speed is measured on a single NVIDIA GeForce RTX 2080 Ti GPU. As seen, LOCATER is much faster than existing LVS methods, owing to its memory-augmented fully attentional architecture design.

TABLE 4
Quantitative results on J-HMDB-S [2] (§5.2).

Method	Backbone	Overlap					mAP 0.5:0.95	IoU	
		P@0.5	P@0.6	P@0.7	P@0.8	P@0.9		Overall	Mean
†Hu <i>et al.</i> [26] [ECCV16]	VGG-16 [116]	63.3	35.0	8.5	0.2	0.0	17.8	54.6	52.8
†Li <i>et al.</i> [48] [CVPR17]	VGG-16 [116]	57.8	33.5	10.3	0.6	0.0	17.3	52.9	49.1
Gavrilyuk <i>et al.</i> [2] [CVPR18]	I3D [5]	71.2	51.8	26.4	3.0	0.0	26.7	55.5	57.0
Wang <i>et al.</i> [3] [ICCV19]	I3D [5]	75.6	56.4	28.7	3.4	0.0	28.9	57.6	58.4
Wang <i>et al.</i> [7] [AAAI20]	I3D [5]	74.2	58.7	31.6	4.7	0.0	30.1	55.4	57.6
McIntosh <i>et al.</i> [8] [CVPR20]	I3D [5]	67.7	51.3	28.3	5.1	0.0	26.1	53.5	55.0
Ning <i>et al.</i> [6] [IJCAI20]	I3D [5]	69.1	57.2	31.9	6.0	0.1	29.4	-	-
Hui <i>et al.</i> [16] [CVPR21]	I3D [5]	78.3	63.9	37.8	7.6	0.0	33.5	59.8	60.4
Yang <i>et al.</i> [19] [BMVC21]	ResNet-101 [117]	81.9	73.6	54.2	16.8	0.4	-	65.2	62.7
LOCATER	*ViT-B [106]	89.3	77.2	50.8	10.6	0.2	36.3	67.3	66.3
MTTR [23] [CVPR22]	Video-Swin-T [118]	93.9	85.2	61.6	16.6	0.1	39.2	70.1	69.8
ReferFormer [22] [CVPR22]	Video-Swin-T [118]	93.3	84.2	61.4	16.4	0.3	39.1	70.0	69.3
LOCATER	Video-Swin-T [118]	93.6	85.9	61.9	16.8	0.3	39.4	70.8	69.6

TABLE 5
Quantitative results on R-YTVOS_{val} [4] (§5.3).

Method	Backbone	$\mathcal{J}\&\mathcal{F}$	\mathcal{J}	\mathcal{F}
Seo <i>et al.</i> [4] [ECCV20]	ResNet-50 [117]	48.9	47.0	50.8
Hui <i>et al.</i> [16] [CVPR21]	I3D [5]	36.7	35.0	38.5
Li <i>et al.</i> [120] [AAAI22]	ResNet-50 [117]	48.6	47.5	49.7
LOCATER	*ViT-B [106]	50.0	48.8	51.1
MTTR [23] [CVPR22]	Video-Swin-T [118]	55.3	54.0	56.6
ReferFormer [22] [CVPR22]	Video-Swin-T [118]	56.0	54.8	57.3
LOCATER	Video-Swin-T [118]	56.5	54.8	58.1

5.2 Results on J-HMDB-S Dataset

To investigate the generalization ability of LOCATER, we also report the performance of our A2D-S trained model on J-HMDB-S [2], following [2], [6]–[8].

Dataset. J-HMDB-S contains 928 short videos with 21 different action categories and 928 language descriptions.

Quantitative Performance. Table 4 presents performance comparison on J-HMDB-S. All models are trained under the same setting on A2D-S_{train} exclusively without fine-tuning. As seen, our model surpasses other competitors across most metrics. Notably, LOCATER yields Mean IoU 66.3%, Overall IoU 67.3% and mAP 36.3%, while the corresponding scores for the previous SOTA method [22] are 62.7%, 65.2% and 33.5%, respectively. Compared with the recent works [22], [23], competitive performance is also achieved. These results confirm again the effectiveness of our LOCATER.

5.3 Results on R-YTVOS Dataset

We further train and test our model on a recently new proposed large-scale dataset, R-YTVOS [4].

Dataset. R-YTVOS has 3,978 videos, with 131K segmentation masks and 15K expressions. Only 3,471/202 train/val videos are public available for training and evaluation.

Quantitative Performance. Following the official leaderboard, we report experimental results of LOCATER along with the SOTA LVS models [4], [16], [120] and two concurrent works [22], [23] in Table 5. We observe that LOCATER

still performs well on this large-scale dataset. LOCATER consistently outperforms these methods on all metrics with the new SOTA scores, *i.e.*, 56.5%/ 54.8%/58.1% $\mathcal{J}\&\mathcal{F}/\mathcal{J}/\mathcal{F}$.

5.4 Qualitative Analysis on A2D-S and R-YTVOS

Fig. 5 depicts visual comparison results on A2D-S_{test} (left) and Refer-Youtube-VOS_{val} (right). LOCATER produces more precise segmentation results against ACGA [3] and CSTM [16]. It shows strong robustness in handling occlusions and complex textual descriptions, especially when facing ambiguity caused by scene dynamics, where the referent is hard to locate relying on narrowly local perspective. Particularly as shown in Fig. 5 (left), beyond the *jump* action, ACGA (1st row, 3rd column) and CSTM (3rd row, 4th column) both fail to distinguish the two actors.

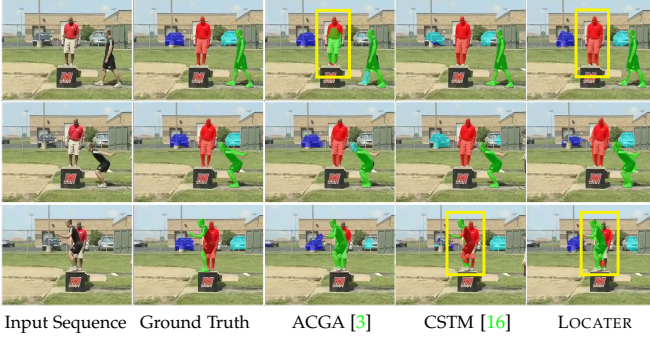
5.5 Results on Our A2D-S⁺ Dataset

Dataset. Basically, A2D-S_M⁺, A2D-S_S⁺, and A2D-S_T⁺ yield increased challenges by collecting or synthesizing videos with multiple objects/actors. For A2D-S_M⁺, it is a subset of A2D-S_{test}, which contains 257 videos with multiple actors. For A2D-S_S⁺ and A2D-S_T⁺, they are built upon the concept of *contrasting* examples [13] (*cf.* §4.1), *i.e.*, videos that are similar to but not exactly the same as described by the language query. They contain 1,290/1,293 distinct videos with 1,295/1,295 linguistic queries respectively.

Quantitative Performance. Our A2D-S⁺ dataset is only used for evaluation. All the benchmarked methods are the ones in Table 3 trained on A2D-S_{train} set. As shown in Table 6, although [3], [16] obtain compelling performance on A2D-S and J-HMDB-S (*cf.* Table 3-4), they cannot handle our challenging cases well. In contrast, our LOCATER yields better overall performance, especially on mIoU (3.2% averaged improvement over all subsets), verifying its strong ability in fine-grained visual-linguistic understanding.

Performance over Varied Number of Objects. Furthermore, for a thorough evaluation, we study the model performance with varied numbers of objects. For either A2S-S_S⁺ or A2S-S_T⁺, we group the generated examples into three clusters according to the number of existing objects, and report the

1. Man in red shirt standing in the middle
2. Man in black jumping up and down
3. Dark colored car on the left
4. Silver car parking on the far right



1. The black and white zebra is on the left in the grass with its head down
2. A zebra to the right of the frame, in front of the other zebra
3. A black and white zebra is in the back on the right behind another looking towards the left

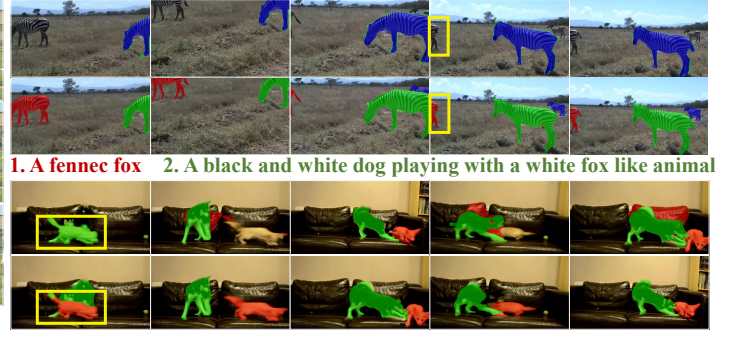


Fig. 5. **Visual comparison results** (§5.4) on A2D-S *test* [2] (left) and R-YTVOS *val* [4] (right). Referents and corresponding descriptions are highlighted in the same colour. In right column, we show qualitative results of CSTM [16] (1st row) and LOCATER (2nd row).

TABLE 6

Quantitative results on A2D-S⁺. LOCATER_{IMG} refers to LOCATER without using memory (§5.5).

Method	A2D-S _M ⁺			A2D-S _S ⁺			A2D-S _T ⁺		
	mAP	oIoU	mIoU	mAP	oIoU	mIoU	mAP	oIoU	mIoU
[3] ICCV19	16.0	45.3	37.2	9.7	25.3	20.1	11.1	29.8	24.4
[16] CVPR21	26.7	50.6	43.3	16.3	34.1	28.7	19.2	38.3	27.5
LOCATER _{IMG}	31.0	52.8	46.5	17.8	30.0	28.4	23.0	35.9	29.7
LOCATER	33.6	54.5	49.0	19.0	31.4	29.9	23.6	37.0	30.2

TABLE 7

Quantitative results with different number of objects. Results are reported in terms of mIoU. LOCATER_{IMG} refers to LOCATER without using memory (§5.5).

#Objets/vid	1	2.40	2.39	4.11	4.19	8.56	8.79
Concatenation	-	Spat-	Temp-	Spat-	Temp-	Spat-	Temp-
[3] ICCV19	69.8	29.9	34.2	19.5	25.0	11.1	13.9
[16] CVPR21	77.0	40.0	36.9	28.8	27.7	17.2	17.4
LOCATER _{IMG}	76.5	39.7	37.6	28.2	29.9	17.1	21.4
LOCATER	77.9	40.8	38.1	29.8	30.4	19.2	22.2

benchmarked results in Table 7. The performance on the single actor subset of A2D-S *test* is also provided for reference. As seen, as the number of semantically similar objects increases, the dataset difficulty also gradually elevated. Yet, the performance gap between LOCATER and other competitors becomes even larger, which well verifies the strong grounding ability of LOCATER.

5.6 Results on RVOS Track in YTB-VOS₂₁ Challenge

Experimental Setup. We first detail the experimental setup for the challenge dataset in YTB-VOS₂₁.

- *Dataset:* R-YTVOS [4] (cf. §5.3) is the standard benchmark. Challenge solutions are first developed on the *test-dev* set, which contains the same video sequences as R-YTVOS *val*, and finally evaluated on the private *test-challenge* set, which contains 305 videos.
- *Evaluation Metric:* Following the official evaluation metrics, we use $J&F$, J and F to evaluate our model.

2. <https://youtube-vos.org/challenge/2021/leaderboard/>

TABLE 8

Benchmarking results on *test-dev* set of RVOS track in YTB-VOS₂₁ challenge [14] (§5.6).

Team	$J&F \uparrow$	$J \uparrow$	$F \uparrow$
LOCATER (Ours)	59.5	57.8	61.1
leonnop (Ours)	61.4 $\uparrow 6.6$	60.0 $\uparrow 6.3$	62.7 $\uparrow 6.7$
nowherespyfly [121]	54.8	53.7	56.0
seonguk [4]	48.9	47.0	50.8
wangluting	48.5	47.1	49.9

TABLE 9

Benchmarking results on *test-challenge* set² of RVOS track in YTB-VOS₂₁ challenge [14] (§5.6).

Team	$J&F \uparrow$	$J \uparrow$	$F \uparrow$
leonnop (Ours)	60.7 $\uparrow 11.3$	59.4 $\uparrow 11.0$	62.0 $\uparrow 11.7$
nowherespyfly [121]	49.4	48.4	50.3
feng915912132	48.2	47.4	49.0
Mercil	41.2	40.6	41.8

- *Implementation Details:* We resize video frames to 384×384 and separate them with a patch size $O = 8$, which results in $N_v = 2, 304$. The linguistic encoder \mathcal{E}_w is implemented as BERT_{BASE} [111]. Our model is trained with an initial learning rate 2×10^{-4} which decays polynomially [109], batch size 48, weight decay 1×10^{-4} and max epoch 50. During testing, we adopt multi-scale inference with horizontal flip and scales of $[0.5, 0.75, 1.0, 1.25, 1.5, 1.75]$. Other settings are kept unchanged (cf. §3.3).

Modifications. In addition to the common challenges in LVS benchmarks, we observe a unique issue in YTB-VOS₂₁: A part of objects in the *test-challenge* set belongs to novel categories that are unseen in the *train* set. Thus, along with the LOCATER trained on YTB-VOS₂₁ challenge dataset, we further ensemble other RES models, *i.e.*, MCN [47], which are trained on open-set data sources, including image-level datasets like RefCOCO [40], RefCOCOg [40] and RefCOCO+ [122]. To effectively combine these predictions, we propose a standalone grounding module. Specifically, the grounding module takes several sequence-level mask predictions as inputs and predicts the similarity scores

TABLE 10
A set of ablation studies (§5.7) on A2D-S_{test} and A2D-S₊. We report the average score on all three subsets of A2D-S₊.

\mathcal{E}_{vw} (§3.2.1)	\mathcal{M} (§3.2.2)	DSL (§3.2.3)	mIoU		\mathcal{E}_{vw} (§3.2.1)	mIoU		N_l	0	N_v	$1.5N_v$	$2N_v$	$3N_v$
			A2D-S	A2D-S ⁺		A2D-S	A2D-S ⁺	N_g					
			47.3	27.0	K=1	58.4	35.2	0	34.8	35.2	35.4	35.4	35.5
✓			54.6	30.8	K=2	59.0	35.8	N_v	35.3	35.5	35.8	36.0	36.1
✓	✓		57.5	35.0	K=3	59.7	36.4	$1.5N_v$	35.3	35.6	36.1	36.4	36.4
✓		✓	57.2	34.8	K=4	59.5	36.4	$2N_v$	35.4	35.8	36.2	36.4	36.4
✓	✓	✓	59.7	36.4	K=5	59.7	36.4	$3N_v$	35.4	35.9	36.2	36.4	36.4

(a) Key components

\mathcal{E}_v (§3.2.1)	mIoU		Query embedding q (§3.2.3)	mIoU		Mode (Eq. 11)	A2D-S	A2D-S ⁺
	A2D-S	A2D-S ⁺		A2D-S	A2D-S ⁺			
I3D [5]	58.3	35.2	Text-invented	58.7	35.7	Encoder only	56.8	34.1
Transformer	59.7	36.4	Visual-guided	59.7	36.4	Cosine distance	59.2	36.3
						Product distance	59.7	36.4

(d) Visual encoder

# Frame	15	30	50	80	100	Interval (#Frame)	3	5	7	10	12	15	20	30
Transformer-style	2.01	2.95	4.57	8.48	11.54	A2D-S	59.7	59.7	59.7	59.7	59.6	59.4	59.3	59.0
LOCATER (Memory)	1.71	2.00	2.22	2.26	2.26	A2D-S ⁺	36.4	36.4	36.4	36.4	36.4	36.1	35.9	35.5

(e) Contextualized query embedding

(f) Decoding mode (mIoU)

(g) Efficiency comparison

(h) Frame sampling interval (mIoU)

based on the referring expression. It is implemented as four stacked Transformer blocks [12] followed by one MLP layer for score prediction. This module complements the precise segmentation masks from LOCATER with novel yet coarse object masks from other models.

Quantitative Results. In Table 8 and 9, we respectively report the final results of our final solution and other top-leading teams on the *test-dev* and *test-challenge* sets of the RVOS track in YTB-VOS₂₁. For completeness, in Table 8, we also report the performance of LOCATER trained under the same setup to our full solution. Other competitors [121] mainly adopt an image-level referring object grounding strategy and simply generate video-level predictions with a fixed tracking module. They not only neglect the indispensable long-term cues within linguistic expressions but also overlook the intrinsic low-level challenges posed within video sequences; In contrast, our model well-addresses these issues. As seen, our final solution significantly surpasses the second-place solution with a large gap of **11.3%/11.0%/11.7%** in terms of $\mathcal{J}\&\mathcal{F}/\mathcal{J}/\mathcal{F}$ on *test-challenge* set. Notably, LOCATER has already surpassed all other competitors significantly.

5.7 Diagnostic Experiments

In this section, we conduct a series of ablative studies on both A2D-S_{test} [2] and our newly proposed A2D-S₊ to fully examine the efficacy of our algorithm design. For A2D-S₊, the score is reported as the average over all the three subsets, *i.e.*, A2D-S_M⁺, A2D-S_S⁺ and A2D-S_T⁺.

Key Component Analysis. To study the effect of essential components of LOCATER, we first establish a baseline, that only remains single-modal encoders and directly concatenates visual and linguistic features [2], [48], [117] for mask prediction (*i.e.*, the first row in Table 10a). Then we gradually add different modules, *i.e.*, *cross-modality encoder* (\mathcal{E}_{vw}), *local-global memory* (\mathcal{M}), and *deeply-supervised learning* (DSL) strategy, into the baseline. As reported in Table 10a,

all these components indeed boost segmentation and combining them together yields the best performance.

Visual Encoder \mathcal{E}_v . Next, to verify the advantage of our fully attentional model design, we replace Transformer based visual encoder \mathcal{E}_v with traditional I3D [5], the conventional backbone in previous works [3], [7], [16], [19], and observe performance degradation in Table 10d. We further notice that, even with I3D as visual backbone, LOCATER still outperforms existing algorithms, if we compare the results with Table 3, *i.e.*, 58.3% *vs* 56.1% (+2.2%) in terms of mIoU.

Cross-Modality Encoder \mathcal{E}_{vw} . Then we study the efficacy of our cross-modality encoder \mathcal{E}_{vw} design, which has $K=3$ attention-based modules. As shown in Table 10b, the performance increases when stacking more modules ($K: 1 \rightarrow 3$), and then the gain becomes marginal ($K: 3 \rightarrow 5$).

Decoding Mode (Eq. 11). We further study the influence of different decoding modes on performance. We consider two variants: **i)** *encoder only* (*i.e.*, replace the decoder with a MLP based segment head); and **ii)** *cosine distance* (*i.e.*, compute the scalar product between ℓ_2 -normalized query and patch embeddings). As shown in Table 10f, directly removing the decoder triggers a clear performance drop (59.2% \rightarrow 56.8% on A2D-S_{test} in terms of mIoU). Compared with *cosine distance*, we find product distance is more favored: 59.7% *vs* 59.2%. This observation is reconfirmed on A2D-S₊.

Local-Global Memory \mathcal{M} . Table 10c summarizes the impact of the capacity of the local-global memory \mathcal{M} in segmentation. As seen, without using either local ($N_l = 0$) or global memory ($N_g = 0$), or even both ($N_l = 0$ and $N_g = 0$), LOCATER suffers from significant performance drop. With the increase of the local or global memory capacity, the performance is improved but the gain becomes less stark, confirming the value of the learnable memory operations.

Contextualized Query Embedding. In §3.2.3, we generate a compact query embedding q based on visual context (Eq. 10). To investigate such a design, we consider an alternative strategy, *i.e.*, applying self-attention to generate q . As

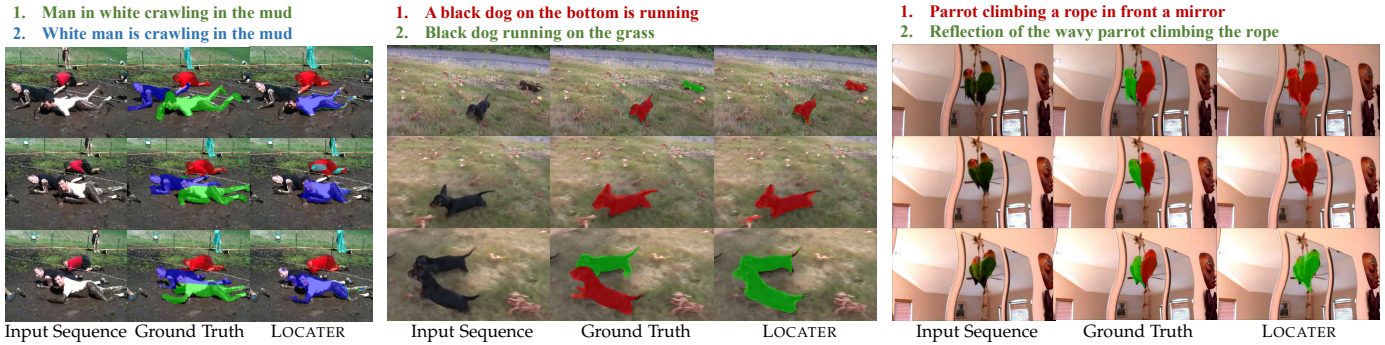


Fig. 6. Typical failure cases on A2D-S $_{\text{test}}$. See §5.8 for more details.

in Table 10e, visual-guided query embedding is more favored. **Efficiency of Memory Design.** We further demonstrate the efficiency of the finite memory design in Table 10g. To clearly reveal the gap, we directly feed image features to both one Transformer block [12] with 12 heads and our memory module (*cf.* §3.2.2). Every frame is patch-wise separated into 256 tokens with 768 feature channels for each. Compared with using conventional Transformer-style network design, *i.e.*, flattening all tokens as input, the advantage of our method in efficiency is more and more significant with the increase of video length.

Frame Sampling Interval. Moreover, we evaluate the impact of frame sampling interval used during global memory construction (§3.2.2). As shown in Table 10h, sampling more frames with smaller intervals (≤ 10) cannot provide performance gain, showing the high redundancy among video frames and explaining the high efficiency of our approach. We, therefore, set the default sampling interval as 10 to construct the global memory \mathcal{M}^g .

5.8 Failure Case Analysis

Despite the stronger cross-modal video understanding ability of LOCATER against previous methods, it still suffers from difficulties in some challenging scenarios. We present three typical failure modes on A2D-S $_{\text{test}}$ in Fig. 6. The *first* type of mistakes is caused by the ambiguity of natural language. For example, in 1st column, LOCATER with an LSTM-based language model, which is trained from scratch, is hard to distinguish the two reference, *i.e.*, *white man* and *man in white*, with limited language training data. This issue can be alleviated by introducing a large-scale pretrained language model, *e.g.*, BERT [111], or harvesting finer language modeling. The *second* type of challenges comes from weak or ambiguous descriptions. For example, in 2nd column, the referent cannot be well differentiated from other objects, as both of the two black dogs are matched well with the query “Black dog running on the grass”. The *third* type of challenges is brought by highly similar referents. For example, in 3rd column, our model faces difficulties in distinguishing the parrot and its reflection, as their appearance and motion information are almost exactly the same.

6 CONCLUSION

This work presents a memory augmented, fully attentional model, LOCATER, for LVS. It effectively aligns cross-modal

representations, and efficiently models long-term temporal context as well as short-term segmentation history through an external memory. With visual context guided expression attention, LOCATER produces frame-specific query vectors for mask generation. We further observe and mitigate the critical absence issue of grounding-required objects in the current most popular A2D-S benchmark with a newly created A2D-S⁺ dataset. It, as a sufficient complement, significantly increases the number of semantically similar objects in testing examples. Experiments demonstrate that LOCATER dramatically advances state-of-the-arts with high efficiency on both standard benchmarks and our proposed challenging A2D-S⁺. Furthermore, our LOCATER based solution achieved the 1st place in RVOS Track of YTB-VOS₂₁ Challenge, surpassing other competitors by large margins.

REFERENCES

- [1] T. Zhou, F. Porikli, D. J. Crandall, L. Van Gool, and W. Wang, “A survey on deep learning technique for video segmentation,” *IEEE Trans. Pattern Anal. Mach. Intell.*, pp. 1–20, 2022.
- [2] K. Gavriluyk, A. Ghodrati, Z. Li, and C. G. Snoek, “Actor and action video segmentation from a sentence,” in *Proc. IEEE Conf. Comput. Vis. Pattern Recognit.*, 2018, pp. 5958–5966.
- [3] H. Wang, C. Deng, J. Yan, and D. Tao, “Asymmetric cross-guided attention network for actor and action video segmentation from natural language query,” in *Proc. IEEE Int. Conf. Comput. Vis.*, 2019, pp. 3938–3947.
- [4] S. Seo, J.-Y. Lee, and B. Han, “Urvos: Unified referring video object segmentation network with a large-scale benchmark,” in *Proc. Eur. Conf. Comput. Vis.*, 2020, pp. 208–223.
- [5] J. Carreira and A. Zisserman, “Quo vadis, action recognition? a new model and the kinetics dataset,” in *Proc. IEEE Conf. Comput. Vis. Pattern Recognit.*, 2017, pp. 4724–4733.
- [6] K. Ning, L. Xie, F. Wu, and Q. Tian, “Polar relative positional encoding for video-language segmentation,” in *Proc. Int. Joint Conf. Artif. Intell.*, 2020, pp. 948–954.
- [7] H. Wang, C. Deng, F. Ma, and Y. Yang, “Context modulated dynamic networks for actor and action video segmentation with language queries,” in *Proc. AAAI Conf. Artif. Intell.*, vol. 34, no. 07, 2020, pp. 12 152–12 159.
- [8] B. McIntosh, K. Duarte, Y. S. Rawat, and M. Shah, “Visual-textual capsule routing for text-based video segmentation,” in *Proc. IEEE Conf. Comput. Vis. Pattern Recognit.*, 2020, pp. 9939–9948.
- [9] X. Lu, W. Wang, J. Shen, D. Crandall, and J. Luo, “Zero-shot video object segmentation with co-attention siamese networks,” *IEEE Trans. Pattern Anal. Mach. Intell.*, vol. 44, pp. 2228–2242, 2020.
- [10] J. Miao, Y. Wei, Y. Wu, C. Liang, G. Li, and Y. Yang, “Vspw: A large-scale dataset for video scene parsing in the wild,” in *Proc. IEEE Conf. Comput. Vis. Pattern Recognit.*, 2021, pp. 4133–4143.
- [11] X. Wang, L. Zhu, Y. Wu, and Y. Yang, “Symbiotic attention for egocentric action recognition with object-centric alignment,” *IEEE Trans. Pattern Anal. Mach. Intell.*, pp. 1–1, 2020.

- [12] A. Vaswani, N. Shazeer, N. Parmar, J. Uszkoreit, L. Jones, A. N. Gomez, L. Kaiser, and I. Polosukhin, "Attention is all you need," in *Proc. Adv. Neural Inf. Process. Syst.*, 2017, pp. 5998–6008.
- [13] A. Sadhu, K. Chen, and R. Nevatia, "Video object grounding using semantic roles in language description," in *Proc. IEEE Conf. Comput. Vis. Pattern Recognit.*, 2020, pp. 10 414–10 424.
- [14] "The 3rd large-scale video object segmentation challenge," <https://youtube-vos.org/challenge/2021/>.
- [15] A. Khoreva, A. Rohrbach, and B. Schiele, "Video object segmentation with language referring expressions," in *Proc. Asian Conf. Comput. Vis.*, 2018, pp. 123–141.
- [16] T. Hui, S. Huang, S. Liu, Z. Ding, G. Li, W. Wang, J. Han, and F. Wang, "Collaborative spatial-temporal modeling for language-queried video actor segmentation," in *Proc. IEEE Conf. Comput. Vis. Pattern Recognit.*, 2021, pp. 4187–4196.
- [17] G. Varol, I. Laptev, and C. Schmid, "Long-term temporal convolutions for action recognition," *IEEE Trans. Pattern Anal. Mach. Intell.*, vol. 40, no. 6, pp. 1510–1517, 2017.
- [18] A. Piergiovanni and M. S. Ryoo, "Learning latent super-events to detect multiple activities in videos," in *Proc. IEEE Conf. Comput. Vis. Pattern Recognit.*, 2018, pp. 5304–5313.
- [19] Z. Yang, Y. Tang, L. Bertinetto, H. Zhao, and P. H. Torr, "Hierarchical interaction network for video object segmentation from referring expressions," in *Proc. Brit. Mach. Vis. Conf.*, 2021.
- [20] Y. Yang, Y. Zhuang, and Y. Pan, "Multiple knowledge representation for big data artificial intelligence: framework, applications, and case studies," *Front. Inf. Technol. Elec. Eng.*, vol. 22, no. 12, pp. 1551–1558, 2021.
- [21] W. Wang and Y. Yang, "Towards data-and knowledge-driven artificial intelligence: A survey on neuro-symbolic computing," *arXiv preprint arXiv:2210.15889*, 2022.
- [22] J. Wu, Y. Jiang, P. Sun, Z. Yuan, and P. Luo, "Language as queries for referring video object segmentation," in *Proc. IEEE Conf. Comput. Vis. Pattern Recognit.*, 2022, pp. 4974–4984.
- [23] A. Botach, E. Zheltonozhskii, and C. Baskin, "End-to-end referring video object segmentation with multimodal transformers," in *Proc. IEEE Conf. Comput. Vis. Pattern Recognit.*, 2022, pp. 4985–4995.
- [24] N. Carion, F. Massa, G. Synnaeve, N. Usunier, A. Kirillov, and S. Zagoruyko, "End-to-end object detection with transformers," in *Proc. Eur. Conf. Comput. Vis.*, 2020, pp. 213–229.
- [25] Y. Wang, Z. Xu, X. Wang, C. Shen, B. Cheng, H. Shen, and H. Xia, "End-to-end video instance segmentation with transformers," in *Proc. IEEE Conf. Comput. Vis. Pattern Recognit.*, 2021, pp. 8741–8750.
- [26] R. Hu, M. Rohrbach, and T. Darrell, "Segmentation from natural language expressions," in *Proc. Eur. Conf. Comput. Vis.*, 2016, pp. 108–124.
- [27] C. Liu, Z. Lin, X. Shen, J. Yang, X. Lu, and A. Yuille, "Recurrent multimodal interaction for referring image segmentation," in *Proc. IEEE Int. Conf. Comput. Vis.*, 2017, pp. 1280–1289.
- [28] H. Shi, H. Li, F. Meng, and Q. Wu, "Key-word-aware network for referring expression image segmentation," in *Proc. Eur. Conf. Comput. Vis.*, 2018, pp. 38–54.
- [29] E. Margffoy-Tuay, J. C. Pérez, E. Botero, and P. Arbeláez, "Dynamic multimodal instance segmentation guided by natural language queries," in *Proc. Eur. Conf. Comput. Vis.*, 2018, pp. 630–645.
- [30] R. Li, K. Li, Y.-C. Kuo, M. Shu, X. Qi, X. Shen, and J. Jia, "Referring image segmentation via recurrent refinement networks," in *Proc. IEEE Conf. Comput. Vis. Pattern Recognit.*, 2018, pp. 5745–5753.
- [31] C. Liang, Y. Wu, T. Zhou, W. Wang, Z. Yang, Y. Wei, and Y. Yang, "Rethinking cross-modal interaction from a top-down perspective for referring video object segmentation," *arXiv preprint arXiv:2106.01061*, 2021.
- [32] L. Ye, M. Rochan, Z. Liu, and Y. Wang, "Cross-modal self-attention network for referring image segmentation," in *Proc. IEEE Conf. Comput. Vis. Pattern Recognit.*, 2019, pp. 10 502–10 511.
- [33] G. Feng, Z. Hu, L. Zhang, and H. Lu, "Encoder fusion network with co-attention embedding for referring image segmentation," in *Proc. IEEE Conf. Comput. Vis. Pattern Recognit.*, 2021, pp. 15 506–15 515.
- [34] T. Hui, S. Liu, S. Huang, G. Li, S. Yu, F. Zhang, and J. Han, "Linguistic structure guided context modeling for referring image segmentation," in *Proc. Eur. Conf. Comput. Vis.*, 2020, pp. 59–75.
- [35] S. Huang, T. Hui, S. Liu, G. Li, Y. Wei, J. Han, L. Liu, and B. Li, "Referring image segmentation via cross-modal progressive comprehension," in *Proc. IEEE Conf. Comput. Vis. Pattern Recognit.*, 2020, pp. 10 485–10 494.
- [36] S. Yang, M. Xia, G. Li, H.-Y. Zhou, and Y. Yu, "Bottom-up shift and reasoning for referring image segmentation," in *Proc. IEEE Conf. Comput. Vis. Pattern Recognit.*, 2021, pp. 11 266–11 275.
- [37] R. Hu, M. Rohrbach, J. Andreas, T. Darrell, and K. Saenko, "Modeling relationships in referential expressions with compositional modular networks," in *Proc. IEEE Conf. Comput. Vis. Pattern Recognit.*, 2017, pp. 4418–4427.
- [38] R. Hu, H. Xu, M. Rohrbach, J. Feng, K. Saenko, and T. Darrell, "Natural language object retrieval," in *Proc. IEEE Conf. Comput. Vis. Pattern Recognit.*, 2016, pp. 4555–4564.
- [39] R. Luo and G. Shakhnarovich, "Comprehension-guided referring expressions," in *Proc. IEEE Conf. Comput. Vis. Pattern Recognit.*, 2017, pp. 3125–3134.
- [40] L. Yu, P. Poirson, S. Yang, A. C. Berg, and T. L. Berg, "Modeling context in referring expressions," in *Proc. Eur. Conf. Comput. Vis.*, 2016, pp. 69–85.
- [41] L. Yu, H. Tan, M. Bansal, and T. L. Berg, "A joint speaker-listener-reinforcer model for referring expressions," in *Proc. IEEE Conf. Comput. Vis. Pattern Recognit.*, 2017, pp. 3521–3529.
- [42] X. Liu, Z. Wang, J. Shao, X. Wang, and H. Li, "Improving referring expression grounding with cross-modal attention-guided erasing," in *Proc. IEEE Conf. Comput. Vis. Pattern Recognit.*, 2019, pp. 1950–1959.
- [43] M. Bajaj, L. Wang, and L. Sigal, "G3graphground: Graph-based language grounding," in *Proc. IEEE Int. Conf. Comput. Vis.*, 2019, pp. 4280–4289.
- [44] P. Wang, Q. Wu, J. Cao, C. Shen, L. Gao, and A. v. d. Hengel, "Neighbourhood watch: Referring expression comprehension via language-guided graph attention networks," in *Proc. IEEE Conf. Comput. Vis. Pattern Recognit.*, 2019, pp. 1960–1968.
- [45] Z. Yang, B. Gong, L. Wang, W. Huang, D. Yu, and J. Luo, "A fast and accurate one-stage approach to visual grounding," in *Proc. IEEE Int. Conf. Comput. Vis.*, 2019, pp. 4682–4692.
- [46] Y. Liao, S. Liu, G. Li, F. Wang, Y. Chen, C. Qian, and B. Li, "A real-time cross-modality correlation filtering method for referring expression comprehension," in *Proc. IEEE Conf. Comput. Vis. Pattern Recognit.*, 2020, pp. 10 877–10 886.
- [47] G. Luo, Y. Zhou, X. Sun, L. Cao, C. Wu, C. Deng, and R. Ji, "Multi-task collaborative network for joint referring expression comprehension and segmentation," in *Proc. IEEE Conf. Comput. Vis. Pattern Recognit.*, 2020, pp. 10 031–10 040.
- [48] Z. Li, R. Tao, E. Gavves, C. G. Snoek, and A. W. Smeulders, "Tracking by natural language specification," in *Proc. IEEE Conf. Comput. Vis. Pattern Recognit.*, 2017, pp. 7350–7358.
- [49] Q. Feng, V. Ablavsky, Q. Bai, and S. Sclaroff, "Siamese natural language tracker: Tracking by natural language descriptions with siamese trackers," in *Proc. IEEE Conf. Comput. Vis. Pattern Recognit.*, 2021, pp. 5851–5860.
- [50] X. Wang, X. Shu, Z. Zhang, B. Jiang, Y. Wang, Y. Tian, and F. Wu, "Towards more flexible and accurate object tracking with natural language: Algorithms and benchmark," in *Proc. IEEE Conf. Comput. Vis. Pattern Recognit.*, 2021, pp. 13 763–13 773.
- [51] S. Caelles, K. Maninis, J. Pont-Tuset, L. Leal-Taixé, D. Cremers, and L. V. Gool, "One-shot video object segmentation," in *Proc. IEEE Conf. Comput. Vis. Pattern Recognit.*, 2017, pp. 5320–5329.
- [52] P. Voigtlaender and B. Leibe, "Online adaptation of convolutional neural networks for video object segmentation," in *Proc. Brit. Mach. Vis. Conf.*, 2017, pp. 116.1–116.13.
- [53] F. Perazzi, A. Khoreva, R. Benenson, B. Schiele, and A. Sorkine-Hornung, "Learning video object segmentation from static images," in *Proc. IEEE Conf. Comput. Vis. Pattern Recognit.*, 2017, pp. 3491–3500.
- [54] V. Jampani, R. Gadde, and P. V. Gehler, "Video propagation networks," in *Proc. IEEE Conf. Comput. Vis. Pattern Recognit.*, 2017, pp. 3154–3164.
- [55] Z. Yang and Y. Yang, "Decoupling features in hierarchical propagation for video object segmentation," in *Proc. Adv. Neural Inf. Process. Syst.*, 2022.
- [56] Z. Yang, Y. Wei, and Y. Yang, "Associating objects with transformers for video object segmentation," in *Proc. Adv. Neural Inf. Process. Syst.*, vol. 34, 2021, pp. 2491–2502.
- [57] W. Wang, J. Shen, F. Porikli, and R. Yang, "Semi-supervised video object segmentation with super-trajectories," *IEEE Trans. Pattern Anal. Mach. Intell.*, vol. 41, no. 4, pp. 985–998, 2018.

- [58] J. S. Yoon, F. Rameau, J. Kim, S. Lee, S. Shin, and I. S. Kweon, "Pixel-level matching for video object segmentation using convolutional neural networks," in *Proc. IEEE Int. Conf. Comput. Vis.*, 2017, pp. 2186–2195.
- [59] W. Wang, J. Shen, X. Lu, S. C. Hoi, and H. Ling, "Paying attention to video object pattern understanding," *IEEE Trans. Pattern Anal. Mach. Intell.*, vol. 43, no. 7, pp. 2413–2428, 2020.
- [60] X. Lu, W. Wang, J. Shen, D. J. Crandall, and L. Van Gool, "Segmenting objects from relational visual data," *IEEE Trans. Pattern Anal. Mach. Intell.*, vol. 43, no. 11, pp. 7885–7897, 2021.
- [61] Z. Yang, Y. Wei, and Y. Yang, "Collaborative video object segmentation by multi-scale foreground-background integration," *IEEE Trans. Pattern Anal. Mach. Intell.*, vol. 44, pp. 4701–4712, 2021.
- [62] X. Lu, W. Wang, M. Danelljan, T. Zhou, J. Shen, and L. Van Gool, "Video object segmentation with episodic graph memory networks," in *Proc. Eur. Conf. Comput. Vis.*, 2020, pp. 661–679.
- [63] J. Lei, L. Wang, Y. Shen, D. Yu, T. L. Berg, and M. Bansal, "Mart: Memory-augmented recurrent transformer for coherent video paragraph captioning," in *Proc. Annu. Meet. Assoc. Comput. Linguist.*, 2020, pp. 2603–2614.
- [64] V. Gabeur, C. Sun, K. Alahari, and C. Schmid, "Multi-modal transformer for video retrieval," in *Proc. Eur. Conf. Comput. Vis.*, 2020, pp. 214–229.
- [65] A. Miech, J.-B. Alayrac, I. Laptev, J. Sivic, and A. Zisserman, "Thinking fast and slow: Efficient text-to-visual retrieval with transformers," in *Proc. IEEE Conf. Comput. Vis. Pattern Recognit.*, 2021, pp. 9826–9836.
- [66] A. U. Khan, A. Mazaheri, N. D. V. Lobo, and M. Shah, "Mmftbert: Multimodal fusion transformer with bert encodings for visual question answering," in *Proc. Conf. Empir. Methods Nat. Lang. Process.*, 2020, pp. 4648–4660.
- [67] M. Zhang, Y. Yang, X. Chen, Y. Ji, X. Xu, J. Li, and H. T. Shen, "Multi-stage aggregated transformer network for temporal language localization in videos," in *Proc. IEEE Conf. Comput. Vis. Pattern Recognit.*, 2021, pp. 12 669–12 678.
- [68] J. Lu, D. Batra, D. Parikh, and S. Lee, "Vilbert: Pretraining task-agnostic visiolinguistic representations for vision-and-language tasks," in *Proc. Adv. Neural Inf. Process. Syst.*, 2019, pp. 13–23.
- [69] H. Tan and M. Bansal, "Lxmert: Learning cross-modality encoder representations from transformers," in *Proc. Conf. Empir. Methods Nat. Lang. Process.*, 2019, pp. 5100–5111.
- [70] G. Li, N. Duan, Y. Fang, M. Gong, and D. Jiang, "Unicoder-vl: A universal encoder for vision and language by cross-modal pre-training," in *Proc. AAAI Conf. Artif. Intell.*, 2020, pp. 11 336–11 344.
- [71] Y.-C. Chen, L. Li, L. Yu, A. El Kholy, F. Ahmed, Z. Gan, Y. Cheng, and J. Liu, "Uniter: Universal image-text representation learning," in *Proc. Eur. Conf. Comput. Vis.*, 2020, pp. 104–120.
- [72] W. Su, X. Zhu, Y. Cao, B. Li, L. Lu, F. Wei, and J. Dai, "Vl-bert: Pre-training of generic visual-linguistic representations," in *Proc. Int. Conf. Learn. Represent.*, 2020.
- [73] R. Hu, A. Singh, T. Darrell, and M. Rohrbach, "Iterative answer prediction with pointer-augmented multimodal transformers for textvqa," in *Proc. IEEE Conf. Comput. Vis. Pattern Recognit.*, 2020, pp. 9989–9999.
- [74] V. Murahari, D. Batra, D. Parikh, and A. Das, "Large-scale pre-training for visual dialog: A simple state-of-the-art baseline," in *Proc. Eur. Conf. Comput. Vis.*, 2020, pp. 336–352.
- [75] W. Hao, C. Li, X. Li, L. Carin, and J. Gao, "Towards learning a generic agent for vision-and-language navigation via pre-training," in *Proc. IEEE Conf. Comput. Vis. Pattern Recognit.*, 2020, pp. 13 134–13 143.
- [76] C. Sun, A. Myers, C. Vondrick, K. Murphy, and C. Schmid, "Videobert: A joint model for video and language representation learning," in *Proc. IEEE Int. Conf. Comput. Vis.*, 2019, pp. 7463–7472.
- [77] L. Zhu and Y. Yang, "Actbert: Learning global-local video-text representations," in *Proc. IEEE Conf. Comput. Vis. Pattern Recognit.*, 2020, pp. 8743–8752.
- [78] H. Ding, C. Liu, S. Wang, and X. Jiang, "Vision-language transformer and query generation for referring segmentation," in *Proc. IEEE Int. Conf. Comput. Vis.*, 2021, pp. 16 321–16 330.
- [79] M. Li and L. Sigal, "Referring transformer: A one-step approach to multi-task visual grounding," in *Proc. Adv. Neural Inf. Process. Syst.*, vol. 34, 2021, pp. 19 652–19 664.
- [80] J. Deng, Z. Yang, T. Chen, W. Zhou, and H. Li, "Transvg: End-to-end visual grounding with transformers," in *Proc. IEEE Int. Conf. Comput. Vis.*, 2021, pp. 1769–1779.
- [81] Z. Qin, X. Lu, X. Nie, D. Liu, Y. Yin, and W. Wang, "Coarse-to-fine video instance segmentation with factorized conditional appearance flows," *IEEE/CAA J. Autom. Sinica*, vol. 10, no. 5, pp. 1–17, 2023.
- [82] A. Kamath, M. Singh, Y. LeCun, G. Synnaeve, I. Misra, and N. Carion, "Mdetr-modulated detection for end-to-end multi-modal understanding," in *Proc. IEEE Int. Conf. Comput. Vis.*, 2021, pp. 1780–1790.
- [83] D. E. Rumelhart, G. E. Hinton, and R. J. Williams, "Learning representations by back-propagating errors," *Nature*, vol. 323, no. 6088, pp. 533–536, 1986.
- [84] S. Hochreiter and J. Schmidhuber, "Long short-term memory," *Neural Comput.*, vol. 9, no. 8, pp. 1735–1780, 1997.
- [85] K. Cho, B. van Merriënboer, D. Bahdanau, and Y. Bengio, "On the properties of neural machine translation: Encoder–decoder approaches," in *8th Workshop Syntax Semant. Struct. Stat. Transl.*, 2014, pp. 103–111.
- [86] H. T. Siegelmann and E. D. Sontag, "On the computational power of neural nets," *J. Comput. Syst. Sci.*, vol. 50, no. 1, pp. 132–150, 1995.
- [87] I. Sutskever, O. Vinyals, and Q. V. Le, "Sequence to sequence learning with neural networks," in *Proc. Adv. Neural Inf. Process. Syst.*, vol. 27, 2014.
- [88] A. Nicolicioiu, I. Duta, and M. Leordeanu, "Recurrent space-time graph neural networks," in *Proc. Adv. Neural Inf. Process. Syst.*, vol. 32, 2019.
- [89] L. Li, T. Zhou, W. Wang, L. Yang, J. Li, and Y. Yang, "Locality-aware inter-and intra-video reconstruction for self-supervised correspondence learning," in *Proc. IEEE Conf. Comput. Vis. Pattern Recognit.*, 2022, pp. 8719–8730.
- [90] A. Graves, G. Wayne, and I. Danihelka, "Neural turing machines," *arXiv preprint arXiv:1410.5401*, 2014.
- [91] J. Oh, V. Chockalingam, H. Lee et al., "Control of memory, active perception, and action in minecraft," in *Proc. ACM Int. Conf. Mach. Learn.*, 2016, pp. 2790–2799.
- [92] E. Parisotto and R. Salakhutdinov, "Neural map: Structured memory for deep reinforcement learning," in *Proc. Int. Conf. Learn. Represent.*, 2019.
- [93] H. Wang, W. Wang, W. Liang, S. C. Hoi, J. Shen, and L. V. Gool, "Active perception for visual-language navigation," *Int. J. Comput. Vis.*, vol. 131, pp. 607–625, 2023.
- [94] D. Bahdanau, K. Cho, and Y. Bengio, "Neural machine translation by jointly learning to align and translate," in *Proc. Int. Conf. Learn. Represent.*, 2015.
- [95] J. Weston, S. Chopra, and A. Bordes, "Memory networks," in *Proc. Int. Conf. Learn. Represent.*, 2015.
- [96] S. Sukhbaatar, J. Weston, R. Fergus et al., "End-to-end memory networks," in *Proc. Adv. Neural Inf. Process. Syst.*, 2015.
- [97] R. Child, S. Gray, A. Radford, and I. Sutskever, "Generating long sequences with sparse transformers," *arXiv preprint arXiv:1904.10509*, 2019.
- [98] I. Beltagy, M. E. Peters, and A. Cohan, "Longformer: The long-document transformer," *arXiv preprint arXiv:2004.05150*, 2020.
- [99] A. Katharopoulos, A. Vyas, N. Pappas, and F. Fleuret, "Transformers are rnns: Fast autoregressive transformers with linear attention," in *Proc. ACM Int. Conf. Mach. Learn.*, vol. 119, 2020, pp. 5156–5165.
- [100] S. Wang, B. Z. Li, M. Khabsa, H. Fang, and H. Ma, "Linformer: Self-attention with linear complexity," *arXiv preprint arXiv:2006.04768*, 2020.
- [101] Z. Dai, Z. Yang, Y. Yang, J. Carbonell, Q. V. Le, and R. Salakhutdinov, "Transformer-xl: Attentive language models beyond a fixed-length context," in *Proc. Annu. Meet. Assoc. Comput. Linguist.*, 2019, pp. 2978–2988.
- [102] C. Liang, W. Wang, T. Zhou, and Y. Yang, "Visual abductive reasoning," in *Proc. IEEE Conf. Comput. Vis. Pattern Recognit.*, 2022, pp. 15 565–15 575.
- [103] X. Wang, W. Wang, J. Shao, and Y. Yang, "Lana: A language-capable navigator for instruction following and generation," in *Proc. IEEE Conf. Comput. Vis. Pattern Recognit.*, 2023.
- [104] C.-Y. Lee, S. Xie, P. Gallagher, Z. Zhang, and Z. Tu, "Deeply-supervised nets," in *Proc. Artif. Intell. Stat.*, vol. 38, 2015, pp. 562–570.
- [105] S. Xie and Z. Tu, "Holistically-nested edge detection," in *Proc. IEEE Int. Conf. Comput. Vis.*, 2015, pp. 1395–1403.
- [106] A. Dosovitskiy, L. Beyer, A. Kolesnikov, D. Weissenborn, X. Zhai, T. Unterthiner, M. Dehghani, M. Minderer, G. Heigold, S. Gelly

- et al.*, "An image is worth 16x16 words: Transformers for image recognition at scale," in *Proc. Int. Conf. Learn. Represent.*, 2021.
- [107] Z. Huang, W. Xu, and K. Yu, "Bidirectional lstm-crf models for sequence tagging," *arXiv preprint arXiv:1508.01991*, 2015.
- [108] D. P. Kingma and J. Ba, "Adam: A method for stochastic optimization," in *Proc. Int. Conf. Learn. Represent.*, 2015.
- [109] C. Liang, W. Wang, J. Miao, and Y. Yang, "Gmmseg: Gaussian mixture based generative semantic segmentation models," in *Proc. Adv. Neural Inf. Process. Syst.*, 2022.
- [110] E. Strubell, P. Verga, D. Andor, D. Weiss, and A. McCallum, "Linguistically-informed self-attention for semantic role labeling," in *Proc. Annu. Meet. Assoc. Comput. Linguist.*, 2018, pp. 5027–5038.
- [111] J. Devlin, M.-W. Chang, K. Lee, and K. Toutanova, "Bert: Pre-training of deep bidirectional transformers for language understanding," in *Proc. Annu. Conf. North Am. Chapter Assoc. Comput. Linguist. Hum. Lang. Technol.*, 2018, pp. 4171–4186.
- [112] P. Shi and J. Lin, "Simple bert models for relation extraction and semantic role labeling," *arXiv preprint arXiv:1904.05255*, 2019.
- [113] S. Pradhan, A. Moschitti, N. Xue, H. T. Ng, A. Björkelund, O. Uryupina, Y. Zhang, and Z. Zhong, "Towards robust linguistic analysis using ontonotes," in *Proc. Conf. Comput. Nat. Lang. Learn.*, 2013, pp. 143–152.
- [114] M. Palmer, D. Gildea, and P. Kingsbury, "The proposition bank: An annotated corpus of semantic roles," *Comput. Linguist.*, vol. 31, no. 1, pp. 71–106, 2005.
- [115] P. Qi, Y. Zhang, Y. Zhang, J. Bolton, and C. D. Manning, "Stanza: A python natural language processing toolkit for many human languages," in *Proc. Annu. Meet. Assoc. Comput. Linguist.*, 2020, pp. 101–108.
- [116] K. Simonyan and A. Zisserman, "Very deep convolutional networks for large-scale image recognition," in *Proc. Int. Conf. Learn. Represent.*, 2015.
- [117] K. He, X. Zhang, S. Ren, and J. Sun, "Deep residual learning for image recognition," in *Proc. IEEE Conf. Comput. Vis. Pattern Recognit.*, 2016, pp. 770–778.
- [118] Z. Liu, J. Ning, Y. Cao, Y. Wei, Z. Zhang, S. Lin, and H. Hu, "Video swin transformer," in *Proc. IEEE Conf. Comput. Vis. Pattern Recognit.*, 2022, pp. 3202–3211.
- [119] F. Perazzi, J. Pont-Tuset, B. McWilliams, L. Van Gool, M. Gross, and A. Sorkine-Hornung, "A benchmark dataset and evaluation methodology for video object segmentation," in *Proc. IEEE Conf. Comput. Vis. Pattern Recognit.*, 2016, pp. 724–732.
- [120] D. Li, R. Li, L. Wang, Y. Wang, J. Qi, L. Zhang, T. Liu, Q. Xu, and H. Lu, "You only infer once: Cross-modal meta-transfer for referring video object segmentation," in *Proc. AAAI Conf. Artif. Intell.*, vol. 36, no. 2, 2022, pp. 1297–1305.
- [121] Z. Ding, T. Hui, S. Huang, S. Liu, X. Luo, J. Huang, and X. Wei, "Progressive multimodal interaction network for referring video object segmentation," *The 3rd Large-scale Video Object Segmentation Challenge*, p. 7, 2021.
- [122] J. Mao, J. Huang, A. Toshev, O. Camburu, A. L. Yuille, and K. Murphy, "Generation and comprehension of unambiguous object descriptions," in *Proc. IEEE Conf. Comput. Vis. Pattern Recognit.*, 2016, pp. 11–20.